Table 1 Antecedent infections and initial electrodiagnoses in 159 patients with Guillain–Barré syndrome

	AIDP	AMAN	Unclassified
Campylobacter jejuni, n = 22	5	16	1
Cytomegalovirus/Epstein-Barr virus, n = 14	13	0	1
Others/none, n = 123	37	53	33
Total, n = 159	55	69	35

AIDP = acute inflammatory demyelinating polyneuropathy; AMAN = acute motor axonal neuropathy.

performed within 13 days of the onset of neurologic symptoms. The mean patient age was 38 years (range, 3 to 80 years). Pretreatment serum samples taken during the first 3 weeks after onset were frozen at −80 °C. Patients were considered positive for *C. jejuni* if they had serologic evidence of *C. jejuni* infection and a definite history of a diarrheal illness within the previous 3 weeks of GBS onset.[15]

Infection serologies. Sera from the patients were tested for the presence of immunoglobulin (Ig) G antibodies against *C. jejuni* by ELISA, as described elsewhere.[16] Serum was considered positive when the titer was ≥1:2,000. Anti-*C. jejuni* antibody titers were ≥1:2,000 in 14 (82%) of 17 GBS patients from whom *C. jejuni* had been isolated but had decreased to the normal range within 6 months of the onset of GBS.[16] Antibodies to CMV and EBV were measured commercially (The Special Reference Laboratory Company, Tokyo, Japan). CMV infection was defined as the presence of IgM antibodies in the ELISA, and EBV infection was defined as the presence of high titers of antibodies against early antigens or IgM antibodies against the virus capsid antigen. The cutoff values for anti-CMV and -EBV assays were determined from data of 200 healthy Japanese subjects. We included CMV/EBV-related GBS because GBS subsequent to infections by these viruses has been proved to be typical AIDP.[8,17]

Antiganglioside antibody testing. The same serum samples were tested for the presence of antibodies to GM1, GM1b, GM2, GD1a, GalNAc-GD1a, GD1b, GT1a, and GQ1b by ELISA, as described elsewhere.[18] IgG anti-*C. jejuni* antibody and antiganglioside antibodies were measured by one of authors (M.K.), who was blinded to the clinical information.

Electrophysiology. Nerve conduction studies were done weekly for the first 4 weeks and monthly for the next 5 months by two examiners (S.K. and K.O.) using the same conventional procedures and the same EMG machine (Viking 4, Nicolet Biomedical Japan, Tokyo, Japan). Motor nerve studies were made of the median, ulnar, peroneal, and tibial nerves, including F-wave analyses. Amplitude and duration of compound muscle action potential (CMAP) were measured for the initial negative phase. Antidromic sensory nerve conduction studies were performed in the median, ulnar, and sural nerves. Patients were classified as having AMAN or AIDP based on the published electrodiagnostic criteria.[3] Normal data of nerve conduction parameters were obtained from 101 healthy subjects.

Results. *Infection serology and initial electrodiagnoses.* Table 1 shows the relation between antecedent infections and electrodiagnoses in the first examination. Of the 159 GBS patients, 30 (19%) were positive for anti-*C. jejuni* antibody; of these 30 patients, 22 had a history of diarrhea before the onset of GBS and were determined as having recent *C. jejuni* infection. Only two patients had a positive stool culture for *C. jejuni*. Eleven (7%) were positive for anti-CMV antibody, and three (2%) were positive for anti-EBV antibody. None had positive serology for two or more organisms. By electrodiagnostic criteria, 159 patients were classified with AIDP (n = 55; 35%) or AMAN (n = 69; 43%) or as unclassifiable (n = 35; 22%) based on the results of the first electrodiagnostic studies performed 1 to 13 days (median, 6 days) after neurologic onset.

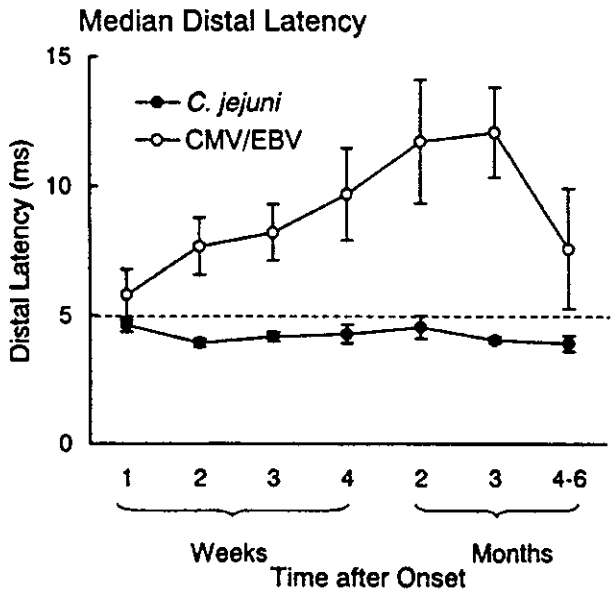

Figure 1. Serial findings of motor distal latencies in the median nerves in patients with infection by cytomegalovirus (CMV)/Epstein–Barr virus (EBV) or Campylobacter jejuni. *The data are given as mean ± SEM. A dotted line indicates the cutoff value of criteria for demyelination.*

Of the 22 *C. jejuni*-positive patients, 16 (73%) were diagnosed with AMAN ($p < 0.01$, compared with the CMV/EBV group), and 5 (23%) showed the AIDP pattern; of these 5 patients, 3 showed prolonged (>120% of upper limits of normal) motor distal latencies in the median and ulnar nerves, and 2 showed prolonged distal latencies in the median, ulnar, and peroneal nerves. None of the five patients had a decrease in conduction velocities and prolonged F-wave latencies, fulfilling the criteria for demyelination. There was no abnormal temporal dispersion or prolonged CMAP duration. Therefore, only prolonged distal latencies met the criteria for demyelination in these patients. One unclassified patient showed mildly reduced CMAP amplitudes, which did not meet the criteria for AMAN (<80% of lower limits of normal).

Of the 14 CMV/EBV-positive patients, 13 (93%) were classified with AIDP ($p < 0.001$, compared with the other patient groups). All 13 patients had prolonged motor distal latencies and F-wave latencies in almost of the nerves tested. The remaining one patient had mild prolongation of distal latencies and F-wave latencies, which did not meet the criteria for AIDP.

Time course of electrodiagnostic findings. Because the electrodiagnosis of AIDP in all 5 *C. jejuni*-positive patients was based on the prolonged distal latencies, we analyzed serial findings of the median distal latencies; figure 1 shows the sequential data in the 22 *C. jejuni*-positive and 14 CMV/EBV-positive patients. The mean latency of the *C. jejuni*-positive group was slightly prolonged during week 1, but there was no significant prolongation in the 6 months after onset of GBS. In contrast, there was a progressive increase in the mean distal latency through month 2 or 3 in the CMV/EBV-positive group. Analysis of ulnar nerve

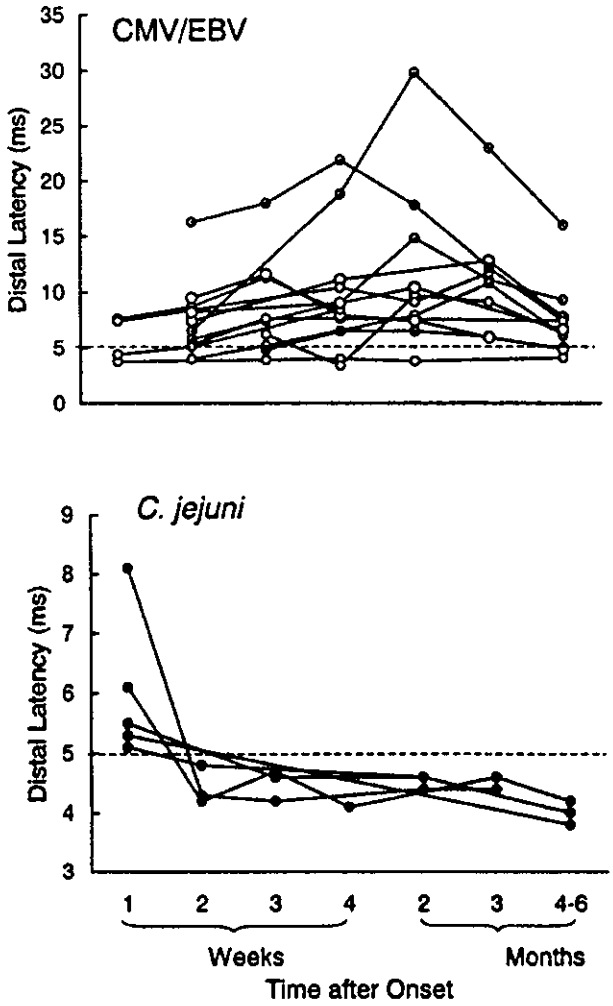

Figure 2. Serial findings of median distal latencies in patients with infection by cytomegalovirus (CMV)/Epstein–Barr virus (EBV) or Campylobacter jejuni. *A dotted line indicates the cutoff value of criteria for demyelination.*

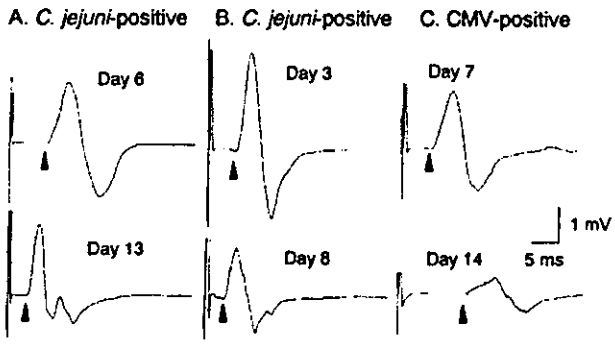

Figure 3. Compound muscle action potentials after median nerve stimulation at the wrist in patients with positive serology for Campylobacter jejuni *(A, B) or cytomegalovirus (CMV; C). Despite similar prolongations of distal latencies during week 1, note rapid shortening within days in* C. jejuni*-positive patients in contrast to a progressive increase in distal latency in a CMV-positive patient (C).*

studies showed similar differences in the time course of distal latencies.

Figure 2 shows distal latency of the median nerve in patients who were classified with AIDP in the first studies. In all five *C. jejuni*-positive patients, the distal latency returned toward normal within 2 weeks. Representative waveforms of CMAPs are shown in figure 3. There were similar increases in distal latencies for *C. jejuni*-positive and CMV-positive patients during week 1. However, the time courses were distinct; the prolonged distal latencies quickly returned toward normal in *C. jejuni*-positive patients but progressively increased in the CMV-positive patient. In the *C. jejuni*-positive patients, CMAP amplitudes after distal stimulation were already low (<80% of lower limit of normal) during week 1, and after normalization of prolonged distal latencies in week 2, these patients were reclassified with AMAN according to the electrodiagnostic criteria.[3]

Features of C. jejuni*-positive patients with the initial diagnosis of AIDP.* Table 2 shows clinical profiles of patients with *C. jejuni* infection who were classified with AIDP in the first studies. All five patients had diarrhea preceding the onset of GBS. Sensory nerve involvement was found for only one patient. These features were consistent with those of AMAN.[19] In the follow-up electrodiagnostic studies during week 2 or 3, four (Patients 1 through 4) were diagnosed with AMAN, and their sensory nerve conduction was normal. Patient 5 was classified with acute motor-sensory axonal neuropathy (AMSAN) because, besides the AMAN pattern in motor nerve studies, the amplitudes of sensory nerve action potentials were decreased in the median, ulnar, and sural nerves. Therefore, none of the *C. jejuni*-positive patients had the time course of typical AIDP in serial electrodiagnostic studies, and all had the final electrodiagnosis of AMAN/AMSAN. All five patients had elevated serum antibodies against gangliosides GM1, GM1b, GD1a, or GalNAc-GD1a. In contrast, none of the 14 CMV/EBV-positive patients had these antibodies, but 3 CMV-positive patients were positive for anti-GM2 IgM antibodies.

Discussion. Our results showed that in this Japanese series 23% of 22 *C. jejuni*-positive patients, who were selected using strict criteria, had the AIDP pattern in the first electrophysiologic studies. The electrodiagnosis was based on the prolonged distal motor latencies, but the distal conduction slowing rapidly returned toward normal, and sensory nerve conduction was normal in almost of them. The time course of nerve conduction abnormality was distinct from that of CMV/EBV-positive AIDP; therefore, demyelination is unlikely to be responsible for the conduction abnormalities. These results suggest that *C. jejuni* infection does not appear to elicit AIDP.

Isolation of *C. jejuni* from stool culture is the gold standard for the diagnosis of infection by this bacterium, but culture survey would underestimate the frequency of *C. jejuni* infection because the time between the infection and GBS onset often exceeds the duration of excretion of viable *C. jejuni* in stools.[20]

Table 2 Profiles of patients with Campylobacter jejuni *infection and initial electrodiagnosis of AIDP*

Patient no.	Age, y/sex	Infectious symptom	Hughes grade	Cranial nerve palsy	Sensory deficit	Final electrodiagnosis	IgG antibody to
1	32/M	Diarrhea	2	Facial, bulbar	—	AMAN	GM1
2	20/M	Diarrhea	2	—	—	AMAN	GM1, GM1b
3	32/F	Diarrhea	1	—	—	AMAN	GM1, GalNAc-GD1a
4	48/M	Diarrhea	2	—	—	AMAN	GM1, GM1b
5	44/M	Diarrhea	4	Facial, bulbar	Yes	AMSAN	GM1, GD1a

AIDP = acute inflammatory demyelinating polyneuropathy; AMAN = acute motor axonal neuropathy; AMSAN = acute motor-sensory axonal neuropathy; — = none; Ig = immunoglobulin.

Serologic studies are more sensitive but less specific than culture-based methods. There are no standards for serologic testing for *C. jejuni* infection with regard to antigens used or cutoff values for the positivity, and the sensitivity and specificity of serologic assays vary considerably among laboratories.[21] The specificity of our assay was 88%,[16] and in combination of a clinical history of a definite diarrheal illness, the strict criteria in this study could reduce the false-positive cases.[15] We suggest that the frequency of *C. jejuni*-related AIDP in previous studies could, in part, be affected by the low specificity of serologic assays and by the lack of analyses of serial electrodiagnostic findings. In a recent report investigating Chinese GBS patients with anti-GalNAc-GD1a or GM1b antibodies, *C. jejuni* serology measured by the same investigator (M.K.) was positive for 54% of 28 AMAN patients and for none of 9 AIDP patients, supporting the view that *C. jejuni* infection is not associated with AIDP.[22]

The blood-nerve barrier is anatomically deficient in the distal nerve terminals and nerve roots,[23] and these regions are preferentially involved in AIDP and AMAN.[24,25] Therefore, conduction slowing or block in the distal nerve segments is the most frequent nerve conduction abnormality in GBS. A number of factors other than demyelination can cause slowing of nerve conduction, such as loss of the fastest fibers, membrane hyperpolarization or depolarization, and sodium channel inactivation.[26] Axonal degeneration of the fast fibers is unlikely to explain prolonged distal latencies seen in our *C. jejuni*-positive patients because motor nerve conduction velocities were normal in those patients, and their rapid normalization is against this view. A previous report studying axonal excitability in GBS suggests that resting membrane potential is not altered in AIDP and AMAN.[27] We speculate that sodium channel dysfunction explains the prolonged distal latencies and their quick reversal in *C. jejuni*-positive patients: in patients with poisoning of tetrodotoxin, which specifically inactivates voltage-gated sodium channels, profound slowing of nerve conduction became normal within days.[28] Moreover, recent electrophysiologic studies in AMAN patients suggest sodium channel dysfunction in the motor nerve terminals,[27,29] possibly mediated by antibodies, cytokines, or other inflammatory substances, although our data could not provide direct evidence of physiologic conduction failure at the nodes of Ranvier.

In almost all of our *C. jejuni*-positive patients with prolonged distal latencies, sensory nerve conduction was normal, and this supports the view that these patients had axonal GBS rather than AIDP because sensory nerve fibers are usually involved in AIDP.[6] Although our study included only Japanese patients and the possibility of host susceptibility factors could not be excluded, based on the clinical and electrophysiologic findings found in this study, we suggest that slowing of motor nerve conduction in *C. jejuni*-positive patients is not caused by segmental demyelination, and, therefore, *C. jejuni* infection does not cause typical AIDP.[30] Patients with axonal GBS can show transient conduction slowing, mimicking one caused by demyelination in the early phase of the illness.[31] In this regard, electrophysiologic classification of GBS would be better determined based on sequential findings rather than on results of single studies.

References

1. Feasby TE, Gilbert JJ, Brown WF, et al. An axonal form of Guillain-Barré polyneuropathy. Brain 1986;109:1115–1126.
2. Griffin JW, Li CY, Ho TW, et al. Guillain-Barré syndrome in northern China: the spectrum of neuropathological changes in clinically defined cases. Brain 1995;118:577–595.
3. Ho TW, Mishu B, Li CY, et al. Guillain-Barré syndrome in northern China: relationship to *Campylobacter jejuni* infection and anti-glycolipid antibodies. Brain 1995;118:597–605.
4. Prineas JW. Pathology of the Guillain-Barré syndrome. Ann Neurol 1981;9:6–19.
5. Hadden RDM, Cornblath DR, Hughes RAC, et al. Electrophysiological classification of Guillain-Barré syndrome: clinical associations and outcome. Ann Neurol 1998;44:780–788.
6. Albers JW, Donofrio PD, McGonagle TK. Sequential electrodiagnostic abnormalities in acute inflammatory demyelinating polyneuropathy. Muscle Nerve 1985;8:528–539.
7. Kuwabara S, Asahina M, Mori M, et al. Two patterns of clinical recovery in Guillain-Barré syndrome with anti-GM1 antibody. Neurology 1998;51:1656–1660.
8. Ogawara K, Kuwabara S, Mori M, et al. Axonal Guillain-Barré syndrome: relation to anti-ganglioside antibodies and *Campylobacter jejuni* infection in Japan. Ann Neurol 2000;48:624–631.
9. Jacobs BC, Rothbarth PH, van der Meché FGA, et al. The spectrum of antecedent infections in Guillain-Barré syndrome: a case control study. Neurology 1998;51:1110–1115.
10. Jacobs BC, van Doorn PA, Schmitz PI, et al. *Campylobacter jejuni* infections and anti-GM1 antibodies in Guillain-Barré syndrome. Ann Neurol 1996;40:181–187.
11. Yuki N, Taki T, Inagaki F, et al. A bacterium lipopolysaccharide that elicits Guillain-Barré syndrome has a GM1 ganglioside-like structure. J Exp Med 1993;178:1771–1775.

12. Yuki N, Taki N, Takahashi M, et al. Penner's serotype 4 of Campylobacter jejuni has a lipopolysaccharide that bears a GM1 ganglioside epitope as well as one that bears GD1a epitope. Infect Immun 1994;62: 2101–2103.
13. Hadden RDM, Karch H, Hartung HP, et al. Preceding infection, immune factors, and outcome in Guillain-Barré syndrome. Neurology 2001;56:758–765.
14. Asbury AK, Cornblath DR. Assessment of current diagnostic criteria for Guillain-Barré syndrome. Ann Neurol 1990;27(suppl):S21–S24.
15. Rees JH, Soudain SE, Gregson NA, Hughes RAC. *Campylobacter jejuni* infection and Guillain-Barré syndrome. N Engl J Med 1995;333:1374–1379.
16. Koga M, Yuki N, Takahashi M, et al. Close correlation of IgA antiganglioside antibodies and antecedent *Campylobacter jejuni* infection in Guillain-Barré and Fisher's syndromes. J Neuroimmunol 1998;81:138–143.
17. Visser LH, van der Meche FGA, Meulstee J, et al. Cytomegalovirus infection and Guillain-Barré syndrome: the clinical, electrophysiologic, and prognostic features. Neurology 1996;47:668–673.
18. Yuki N, Taki T, Handa S. Antibodies to GalNAc-GD1a and GalNAc-GM1b in Guillain-Barré syndrome subsequent to *Campylobacter jejuni* enteritis. J Neuroimmunol 1996;71:155–161.
19. McKhann GM, Cornblath DR, Griffin JW, et al. Acute motor axonal neuropathy: a frequent cause of acute flaccid paralysis in China. Ann Neurol 1993;33:333–342.
20. Nachamkin I, Allos BM, Ho T. *Campylobacter* species and Guillain-Barré syndrome. Clin Microbiol Rev 1998;11:555–567.
21. Koga M, Ang CW, Yuki N, et al. Comparative study on preceding *Campylobacter jejuni* infection in Guillain-Barré syndrome between Japan and the Netherlands. J Neurol Neurosurg Psychiatry 2001;70:693–695.
22. Yuki N, Ho TW, Tagawa Y, et al. Autoantibodies to GM1b and GalNAc-GD1a: relationship to *Campylobacter jejuni* infection and acute motor axonal neuropathy in China. J Neurol Sci 1999;164:134–138.
23. Olsson Y. Microenvironment of the peripheral nervous system under normal and pathological conditions. Crit Rev Neurobiol 1990;5: 265–311.
24. Brown WF, Snow R. Patterns and severity of conduction abnormalities in Guillain-Barré syndrome. J Neurol Neurosurg Psychiatry 1994;54: 768–774.
25. Kuwabara S, Yuki N, Koga M, et al. IgG anti-GM1 antibody is associated with reversible conduction failure and axonal degeneration in Guillain-Barré syndrome. Ann Neurol 1998;44:202–208.
26. Burke D, Kiernan MC, Bostock H. Excitability of human axons. Clin Neurophysiol 2001;112:1575–1585.
27. Kuwabara S, Ogawara K, Sung JY, et al. Differences in membrane properties in axonal and demyelinating Guillain-Barré syndromes. Ann Neurol 2002;52:180–187.
28. Oda K, Araki K, Totoki T, Shibasaki H. Nerve conduction study of human tetrodotoxication. Neurology 1989;39:743–745.
29. Kuwabara S, Bostock H, Ogawara K, et al. The refractory period of transmission is impaired in axonal Guillain-Barré syndrome. Muscle Nerve 2003;23:683–689.
30. Sheikh KA, Nachamkin I, Ho TW, et al. *Campylobacter jejuni* lipopolysaccharides in Guillain-Barré syndrome. Molecular mimicry and host susceptibility. Neurology 1998;51:371–378.
31. Capasso M, Caporale CM, Pomilio F, et al. Acute motor conduction block neuropathy: another Guillain-Barré syndrome variant. Neurology 2003;61:617–622.

Immunoglobulin improves a model of acute motor axonal neuropathy by preventing axonal degeneration

Y. Nishimoto, MD; M. Koga, MD, PhD; M. Kamijo, MD, PhD; K. Hirata, MD, PhD; and N. Yuki, MD, PhD

Abstract— *Background:* The action mechanism of IV immunoglobulin (IVIg) for Guillain-Barré syndrome has yet to be clarified. *Objective:* To evaluate clinical, histologic, and immunologic effects in a disease model of acute motor axonal neuropathy (AMAN) treated by IVIg. *Methods:* Rabbits were sensitized with gangliosides including GM1 and divided randomly into two groups at disease onset. One group received IV homologous γ-globulin (400 mg/kg/day) for 5 days (n = 15), and the other received saline (n = 15). Disease severity was scored (0 to 13 points) daily. Sixty days after onset, anti-GM1 antibodies were tested by ELISA, and the number of degenerative axons was counted in spinal anterior roots. *Results:* Between both groups at onset, there was no difference in any characteristics including clinical score. The IVIg group had faster recovery than the saline group ($p = 0.03$). The percentage of rabbits that improved by a score of ≤4 was higher in the IVIg (53%) than in the saline (13%) group 60 days after onset ($p = 0.03$). Anti-GM1 IgG titers 60 days after onset did not differ between the groups. The anterior roots of rabbits surviving 60 days after onset showed lower frequency of axonal degeneration in the IVIg-treated (n = 11; mean 4.5%) than in the saline-treated (n = 8; mean 11.1%) rabbits ($p = 0.01$). *Conclusions:* The therapeutic efficacy of IVIg in an AMAN model was confirmed. IVIg may not affect the production or catabolism of anti-GM1 IgG, but it may prevent axonal degeneration of motor nerves.

NEUROLOGY 2004;62:1939–1944

Guillain-Barré syndrome (GBS) has been referred to as acute inflammatory demyelinating polyneuropathy (AIDP). This view was shaped in part by what is known of its laboratory analogue, experimental autoimmune neuritis (EAN), induced by immunization with P_2 or P_0 protein (components of peripheral nerve myelin), but neither protein seems to be a target molecule in patients with AIDP.[1,2] An "axonal form of GBS" was proposed in 1986,[3] and later the existence of the axonal variants of GBS, acute motor axonal neuropathy (AMAN) and acute motor–sensory axonal neuropathy, was established.[4-6] We recently established an animal disease model of AMAN,[7] in which the clinical, pathologic, and immunologic features of rabbits are very similar to those of AMAN. On sensitization with bovine brain ganglioside (BBG) mixture, all 13 rabbits developed high anti-GM1 IgG antibody titers and flaccid limb weakness of acute onset and had a monophasic illness course. Pathologic findings for the peripheral nerves showed predominant Wallerian-like degeneration with neither lymphocytic infiltration nor demyelination. IgG was deposited on axons of the anterior roots, and GM1 was shown to be present on axons of the peripheral nerves.

IV immunoglobulin (IVIg) is effective for GBS in shortening recovery time,[8,9] but the action mechanism has not yet been determined. We tested whether IVIg was clinically effective in AMAN rabbits and evaluated how it acts histologically and immunologically. IVIg had a beneficial effect in a rabbit AMAN model, although rat EAN models have provided conflicting results regarding its effects.[10,11]

Additional material related to this article can be found on the *Neurology* Web site. Go to www.neurology.org and scroll down the Table of Contents for the June 8 issue to find the title link for this article.

Materials and methods. *Experiment 1.* Induction of the disease model. Male Japanese white rabbits (2.0 to 2.5 kg; Oriental Bio-Service Kanto, Tsukuba, Ibaraki, Japan) were used. They were caged individually, provided food (commercially available chow) daily, and had unrestricted access to water. The disease model was induced by active immunization by the procedure described elsewhere with minor modification.[7] An emulsion containing 2.5 mg of a BBG mixture (Cronassial; Fidia, Padova, Italy)

From the Department of Neurology (Drs. Nishimoto, Koga, Hirata and Yuki), Dokkyo University School of Medicine, Tochigi, and Department of Neurology (Dr. Kamijo), Labor Welfare Corporation, Chubu Rosai Hospital, Aichi, Japan.

Supported in part by a Grant-in-Aid for Scientific Research (B) (KAKENHI 14370210 to N.Y.) from the Ministry of Education, Culture, Sports, Science, and Technology of Japan and a grant from the Japan Health Sciences Foundation.

Received November 5, 2003. Accepted in final form February 2, 2004.

Address correspondence and reprint request to Dr. N. Yuki, Department of Neurology, Dokkyo University School of Medicine, Kitakobayashi 880, Mibu, Shimotsuga, Tochigi 321-0293, Japan; e-mail: yuki@dokkyomed.ac.jp

Table *Clinical scale and clinical feature frequencies*

Clinical feature	Frequencies, %	
	5 d before onset	At onset
Abnormal posture	10	97
Neck weakness	27	87
Slip of forelimbs	30	70
Slip of hindlimbs	50	80
Dragging forelimbs	0	7
Dragging hindlimbs	0	27
Unable to walk	0	0
Slow righting reflex	3	33
No righting reflex	0	7
Ptosis	0	13
Tremor of limbs or trunk induced by pulling tail	0	33
Spontaneous tremor of limbs or trunk	0	17
Animal appeared systemically unwell	0	0

A score of 1 point was given for each of the 13 clinical features shown in the left column. n = 30.

was injected subcutaneously to the back at 3-week intervals. Active immunization was continued until disease onset or the eighth inoculation. This study was carried out in accordance with the Guidelines for the Care and Use of Laboratory Animals of Dokkyo University School of Medicine, the law concerning Kind Treatment and Management of Animals, and the Japanese government's notification on Feeding and Safe-Keeping of Laboratory Animals. All procedures were approved by the Animal Care and Use Committee (approved no. 0037) of Dokkyo University School of Medicine.

Clinical scale. The clinical scale used was a modification of the scale of the previous study.[10] A score of 1 point was given for each of the 13 clinical features shown in the left column of the table. The observed clinical features were totaled daily to calculate the daily clinical score (maximum score 13). Disease onset was defined as a daily clinical score of ≥4. Death was given the score of 13 until the end of the experiment because it could be considered the severest clinical state.

Protocol of treatment with IVIg. When rabbits fulfilled the criteria for disease onset, they were divided into two groups (Groups A and B) by permuted block randomization with a size 10 block. Group A animals received IV injections of 400 mg/kg (in 4 mL of saline/kg) of rabbit γ-globulin (Serological Proteins, Kankakee, IL) daily from onset for 5 days. Rabbit γ-globulin preparation was derived from the rabbit's plasma by the Cohn cold ethanol fractionation process, as were the human γ-globulin preparations. Homologous γ-globulin was used because in a pilot study, IV human γ-globulin induced anemia and hematuria in several rabbits. Group B animals received the same volume of saline IV for 5 days. The solution was injected slowly over 1 hour by syringe pumps (model 100 series; KD Scientific, Boston, MA). The rabbits were weighed and examined for each clinical sign daily by an observer who was unaware of the treatment allocation. Rabbits were checked daily for 60 days after disease onset and then killed.

Outcome measures. The primary outcome measures were the time from disease onset to death and the mortality rate on day 60 after onset. Secondary outcome measures were the time required to improve to a daily clinical score of ≤4 and the percentage of rabbits with scores of ≤4 at 60 days after onset. Other outcome measures were changes from onset in the daily clinical score and body weight.

Histologic analysis. Five normal rabbits not given active immunization or treatment constituted the histologic controls and were housed for 9 weeks under the same conditions as Groups A and B. After the follow-up period, the normal and disease rabbits were anesthetized deeply with pentobarbital sodium and then perfused transcardially with 3% glutaraldehyde/1% paraformaldehyde as described elsewhere.[7] Lumbar cords with the right spinal roots were excised and immersed in the same fixative. Samples were postfixed with 1% osmium tetroxide, dehydrated in a graded ethanol series, and then embedded in Epon 812 (Polysciences, Warrington, PA). Cross-sections 0.7 μm thick were cut from each sample and stained with 0.5% toluidine blue. Morphologic evaluation of each ventral root was made on olivine blue sections. One of the authors, who was unaware of the clinical information, manually counted the number of degenerative axons from every two to four frame areas (single frame, 0.03 mm^2) in the ventral root of the lumbar cord.[12] The frequency of degenerative axons (the ratio of the number of degenerative axons to the total number of axons of all frame areas) was calculated for each rabbit.

ELISA. Blood samples were taken from each rabbit by ear vein puncture at disease onset and on day 60. Plasma thereafter was stored at −80 °C until used. ELISA with minor modifications used to measure anti-GM1 IgG antibody was reported elsewhere.[13] In brief, 5-pmol samples of GM1 were placed in individual microtiter plate wells. Plasma samples diluted 1:500 were added to the wells, and the plates were incubated at 4 °C overnight. Peroxidase-conjugated anti-rabbit γ-chain-specific antibodies (Nordic, Tilburg, the Netherlands; 1:1,000 dilutions) then were added, and the plates were kept at 20 °C for 2 hours. Color was developed with *o*-phenylenediamine. After 15 minutes, the reaction was stopped with 2 *N* hydrochloride. The absorbance at 492 nm/620 nm (as reference) was measured, and the mean value for triplicate reference wells without antigen was subtracted from the mean value for triplicate sample wells. A colleague blinded to the clinical information then assessed the optical densities. To correct for assay variations, well-characterized rabbit plasma with high anti-GM1 IgG antibody titer was the internal standard.

Experiment 2. Another experiment was performed to determine whether IVIg could inhibit disease onset. At each sensitization with BBG, six rabbits were given IV injections of rabbit γ-globulin (400 mg/kg) daily for 5 days. Treatment was repeated at 3-week intervals until disease onset or the fifth inoculation (Group C). Rabbits in Group C were weighed daily and examined for each clinical sign by an observer. They were followed for 105 days after the first inoculation and then killed. Twenty-seven rabbits (Group D) from Groups A and B, which had fulfilled the criteria for disease onset during the 105 days after the first inoculation, were used as controls. Outcome measures were inoculation times, days from first inoculation to onset, daily clinical score at onset, and weight at onset.

Statistical analysis. Baseline characteristics of the rabbits in Experiment 1 were compared between the groups by the Mann-Whitney *U* test. The Fisher exact test was used for the 2 × 2 tables to compare categorical data. The time to reach clinical endpoint (death or improvement to a score of ≤4) was compared by the Kaplan-Meier method and log-rank test. Mean in changes of the daily clinical score and weight from disease onset were compared by the two-tailed Student *t*-test after each area under the daily clinical score and weight curve from onset was calculated. This analysis was made every 5 days after onset. The Mann-Whitney *U* test was used to compare groups with respect to the daily clinical score and anti-GM1 IgG antibody titers between the same time points. Histologic data for the rabbits surviving on day 60 after onset were analyzed by the Kruskal-Wallis test and Steel-Dwass procedure to verify the difference between two groups. Differences in time between the groups in Experiment 2 were compared using the Mann-Whitney *U* test. Statistical analyses were conducted with Microsoft Excel (Redmond, WA) and SPSS 11.0J (Chicago, IL) software. A p value of <0.05 was considered significant.

Results. *Experiment 1.* Three rabbits were excluded because of unexpected spinal cord injury. Thirty (81%) of the remaining 37 rabbits that had received IVIg (Group A; n = 15) or saline (Group B; n = 15) treatment fulfilled the criteria for disease onset. There was no difference in any characteristics between the groups (see supplementary table 1, available at www.neurology.org).

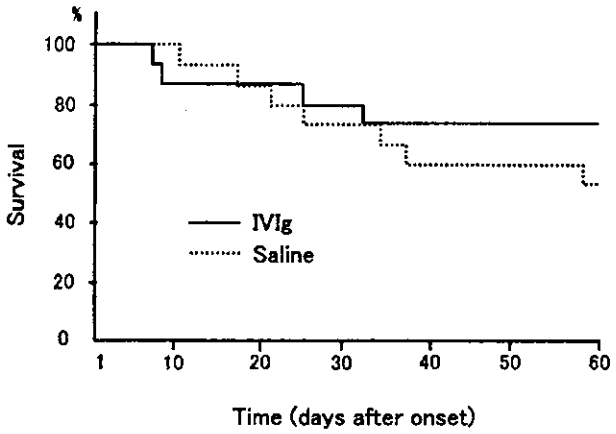

Figure 1. Kaplan-Meier curves showing percentages of rabbits surviving during the 60 days after disease onset. IVIg = IV immunoglobulin.

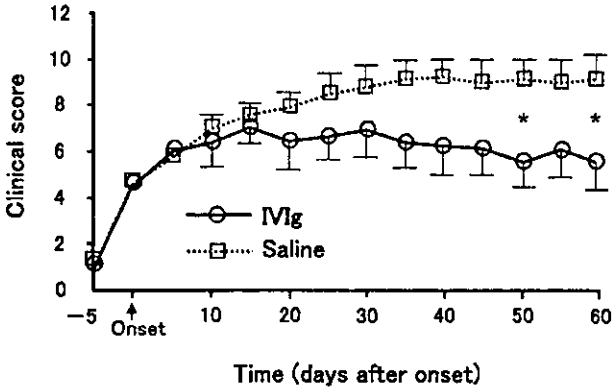

*Figure 3. Changes in the mean clinical score during the 60 days after disease onset (means ± SEM). *Median clinical score significantly differed between Groups A and B. IVIG = IV immunoglobulin.*

Clinical features before and at disease onset. Five days before disease onset, 7 (23%) rabbits had a clinical score of 0, 12 (40%) a score of 1, 9 (30%) a score of 2, and 2 (7%) a score of 3. At onset, 18 (60%) rabbits had a clinical score of 4, 8 (27%) a score of 5, 1 (3%) a score of 6, 1 (3%) a score of 7, and 2 (7%) a score of 8. Four features of the clinical scale (abnormal posture, neck weakness, slip of forelimbs, and slip of hindlimbs) were frequent at disease onset (table). Disease onset in the AMAN rabbits was easily recognized by observing these four features.

Primary outcome. There was no difference in the survival curves of Groups A and B traced by the Kaplan-Meier method (log-rank test, $p = 0.34$) (figure 1). Eleven rabbits had died by day 60 after disease onset: four in Group A and seven in Group B ($p = 0.23$).

Secondary outcome. Kaplan-Meier curves showed faster improvement, a score of ≤4, in Group A than B (log-rank test, $p = 0.03$) (figure 2). The percentage of rabbits showing improvement by a score of ≤4 at 60 days after onset was higher in Group A (53%) than B (13%) (odds ratio [OR] 7.43, 95% CI 1.23 to 45.01, $p = 0.03$).

Other outcomes. Daily clinical scores were lower in Group A than B at 50 days (median 4 [range 0 to 13] points vs median 8 [range 4 to 13] points; $p = 0.01$) and 60 days (median 3 [range 0 to 13] points vs median 8 [range 3 to 13] points; $p = 0.03$) after disease onset (figure 3). There was, however, no difference between Groups A (mean 378.1 points × day; SD 220.3) and B (mean 489.3 points × day; SD 142.2) in daily clinical score, as shown by the area-under-curve values for the daily clinical score (95% CI −27.4 to 249.9, $p = 0.11$) (see figure 3). Mean change of weight for Group A (mean −3.29 g × day; SD 4.06) was less than that for Group B (mean −6.11 g × day; SD 3.30) (95% CI 0.06 to 5.59, $p = 0.046$).

Plasma anti-GM1 IgG antibody. Figure 4 shows that there was no significant difference in anti-GM1 IgG antibody activities between Groups A and B at disease onset. On the day of sacrifice (60 days after onset), there also was no difference between Groups A and B.

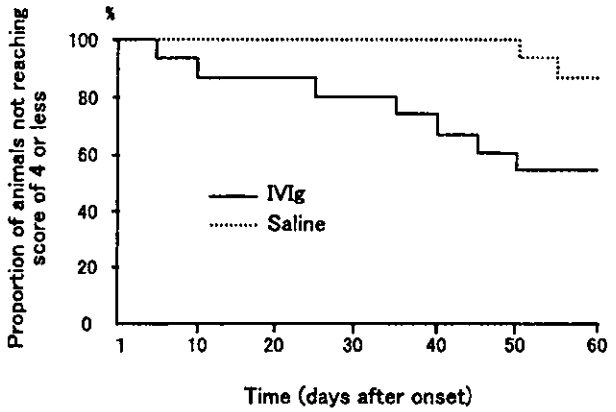

Figure 2. Kaplan-Meier curves showing percentages of animals not reaching a score of ≤4 during the 60 days after disease onset. IVIg = IV immunoglobulin.

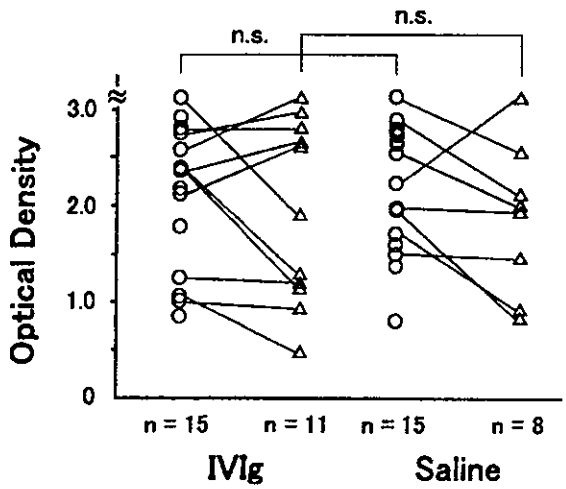

Figure 4. Changes of anti-GM1 IgG antibody activity in the diseased rabbits treated with IV immunoglobulin (IVIg) (Group A) or saline (Group B). The optical density values are shown at the disease onset (circles) and 60 days after the onset (triangles). Paired data of each rabbit are connected by a straight line. n.s. = not significant.

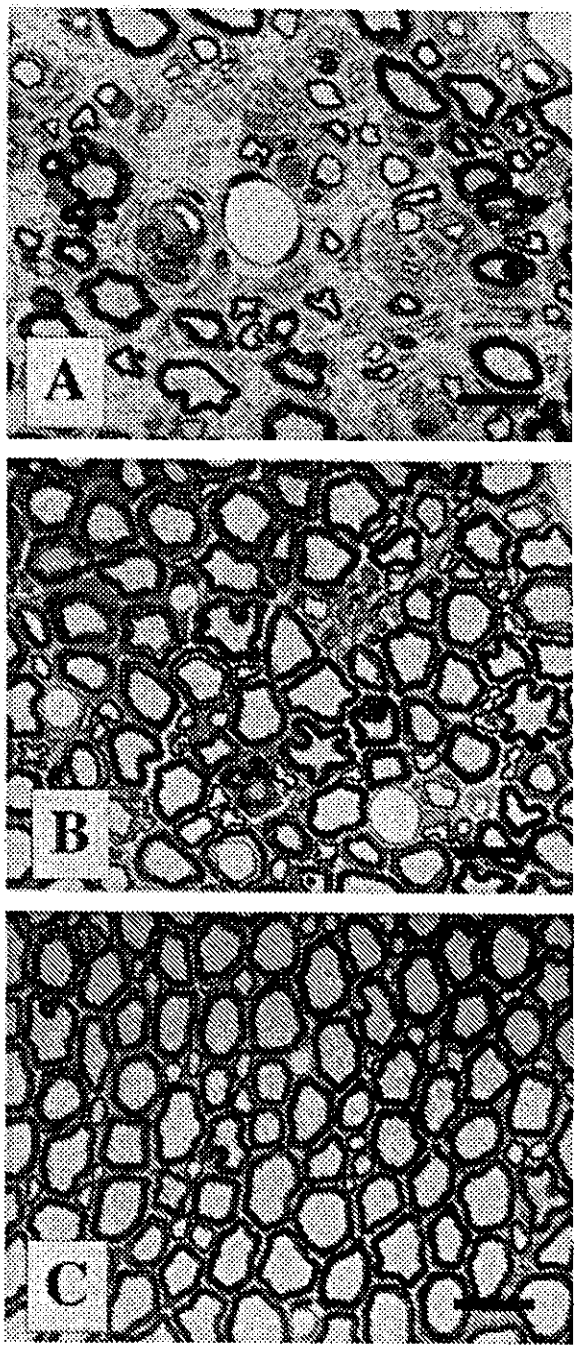

Figure 5. Toluidine blue (0.5%)-stained sections showing lumbar cord ventral roots of disease model rabbits that received saline (A) and IV immunoglobulin (B) and those of untreated normal rabbits (C). Note the extensive axonal degeneration, perineurial edema, and cellular infiltration in the ventral roots of the diseased rabbits. Bar = 20 μm.

Histologic findings. Histologic changes in the ventral roots of the disease rabbits were extensive: axonal degeneration, perineurial edema, and macrophage infiltration of various degrees (figure 5, A and B), whereas there was little histologic change in the ventral roots of the untreated normal rabbits (n = 5; see figure 5C). In the quantitative

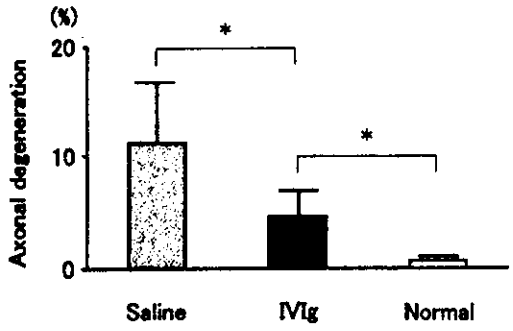

*Figure 6. Mean percentages of axonal degeneration fibers in the ventral roots of the lumbar cord. Frequency of axonal degeneration differed between the groups (*p = 0.01). Statistical analysis was done by the Steel-Dwass test. White column = untreated normal rabbits (n = 5); black column = disease model rabbits given IV immunoglobulin (IVIg) (n = 11); gray column = disease model rabbits given saline (n = 8). Error bar = SD.*

study, the frequency of extensive axonal degeneration differed between the IVIg-treated (n = 11), saline-treated (n = 8), and untreated normal rabbits (Kruskal-Wallis H statistic = 16.4, $df = 2$, $p < 0.01$) (figure 6) groups. Axonal degeneration was less in the IVIg-treated (mean 4.5%; SD 2.7) than saline-treated (mean 11.1%; SD 5.7) group ($p = 0.01$). Clinical scores 60 days after onset also were lower in the IVIg-treated (median 2; range 0 to 7) than saline-treated (median 7; range 3 to 8) group ($p = 0.02$). Normal untreated rabbits had lower frequencies of axonal degeneration (mean 0.7%; SD 0.1) than did the other two groups ($p < 0.01$ in each group).

Experiment 2. All six rabbits in Group C had fulfilled the criteria for disease onset by day 105. The number of days from the first inoculation to disease onset statistically was greater in Group C than D (see supplementary table 2, available at www.neurology.org). There was no difference in the clinical scores at onset between two groups, whereas median weight at onset was significantly higher in Group C.

Discussion. Previous investigations of the effect of human Ig on EAN gave conflicting findings. EAN rats produced by synthetic peptide derived from bovine P_2 protein were treated with IVIg when maximal clinical scores were recorded, but the drug did not alter the course of EAN,[11] whereas human Ig administered intraperitoneally at disease onset accelerated recovery from EAN induced by bovine spinal root myelin.[10] We examined the efficacy of IVIg in AMAN rabbits; although rabbit albumin should be used as a control to confirm it in future studies, our findings verified the usefulness of IVIg and are compatible with results of clinical trials that showed that IVIg produced a shorter time to recovery from GBS.[8,9]

The cauda equina in EAN rats treated with Ig and albumin showed demyelination, axonal degeneration, and remyelination.[10] There was no significant difference in the extent of the changes between the groups, but the proportion of demyelinated fibers

that had started to remyelinate was greater than in the Ig-treated rats. The accelerated rate of recovery of EAN rats treated with Ig may be due to earlier remyelination of demyelinated fibers. In contrast, histologic findings for AMAN rabbits treated with IVIg suggest partial prevention of axonal degeneration in the ventral root. These findings are important for understanding the action mechanism of IVIg, which cannot be obtained from clinical trials and in vitro experiments, although there are potential differences between rabbit and human IVIg.

IVIg treatment of GBS patients with anti-GM1 antibody was reported as superior to plasmapheresis in terms of time to recovery,[14,15] although this could not be confirmed in another study.[16] Electrodiagnosis of a majority patients with GBS who had anti-GM1 IgG showed AMAN,[17] but this finding is controversial for several reasons reported elsewhere.[18] Plasma exchange may have a therapeutic effect by removing circulating factors (Igs, compliments, and cytokines), whereas the action mechanism of IVIg is unclear. Our study, however, showed that IVIg produced less degeneration of motor axons, which may cause faster clinical improvement of GBS patients who had anti-GM1 antibodies, as well as of the AMAN rabbits. Possible mechanisms to prevent axonal degeneration in AMAN are discussed later.

Anti-rat myelin IgG antibody in EAN rats treated at disease onset was significantly less in an Ig- than albumin-treated group,[10] but this difference disappeared 1 week later. The discrepancy is not explained by the turnover of IgG, which has a half-life of 3 weeks. IgG antibody titers against synthetic peptide did not differ between EAN rats with and without IVIg treatment.[11] In our AMAN rabbits 60 days after onset, there was no significant difference in anti-GM1 IgG titers between the IVIg- and saline-treated groups. Whether IVIg can effectively reduce anti-GM1 IgG titer in GBS patients has yet to be investigated, but it did not reduce the anti-GM1 IgM titers of multifocal motor neuropathy patients whose strength improved.[19,20] Anti-idiotypic antibodies in IVIg, discussed hereafter, may affect antibody production by sending negative signals to B cells.[21] The large amount of IgG in an IVIg preparation may saturate the neonatal Fc receptor (FcRn), accelerate the catabolism of endogenous pathogenic IgG, and reduce autoantibody levels.[22] Our findings, however, suggest that neither suppression of anti-GM1 IgG production nor accelerated catabolism of the autoantibody occurred in AMAN rabbits treated with IVIg, and neither IVIg mechanism has importance for the effective treatment of GBS associated with anti-GM1 IgG.

Treatment given from the time of immunization of EAN rats is reported to prevent paralysis in one study,[11] but not in other studies.[10,23] Treatment from immunization statistically took a longer time in AMAN rabbits to produce disease onset, but it did not prevent paralysis. In the previous study,[10] treatment of EAN rats from disease onset was more beneficial than treatment from immunization. The observation period for our AMAN rabbits was too short for comparison because our interest was whether IVIg could prevent paralysis. Their and our results, however, suggest that Ig acts in the late phases of the disease rather than in the initial immunization process.

In AMAN autopsy cases, IgG and the complement activation product were found bound to the axolemma of motor fibers.[24] Although the most frequent deposit site was the nodal axolemma, IgG and C3d also were present in the periaxonal space of myelinated internodes and bound to the outer surface of the motor axon in the more severe cases. Macrophages surround axons in the periaxonal space without damaging the myelin.[6] In AMAN model rabbits, IgG also was deposited on the axon, and periaxonal macrophages were present.[7,25] GM1 is highly expressed on the axons of humans and rabbits.[7,26] The predominant anti-GM1 IgG antibody subclasses in GBS were IgG_1 and IgG_3, which both fix complement.[27,28] A hypothetical immunopathologic sequence of events has been proposed[24]: 1) Anti-GM1 IgG binds to the nodal axolemma, and the complement is fixed. 2) Anti-GM1 IgG and activated complement enter the periaxonal space of the internode and guide macrophages to that space. 3) Anti-GM1 IgG antibody-dependent cytotoxicity or complement- or macrophage-mediated cytotoxicity then induces primary axonal degeneration.

Because IVIg preparations are derived from a large pool of human donors, the IgG molecules in IVIg contain antibodies with a wide range of idiotypic and anti-idiotypic specificities.[21] Infused anti-idiotypic antibodies have the potential to bind to and neutralize pathogenic autoantibodies, thereby preventing their interaction with the autoantigen. Therapeutic IVIg can neutralize the neuromuscular blocking IgG antibodies in GBS.[29] An Fab fragment prepared from the IVIg has been reported to be as effective as complete IVIg.[29] The $F(ab')_2$, but not the Fc portion, of the IgG in IVIg preparations inhibited the binding of anti-GM1 antibodies to GM1-coated microtiter plates and the binding of cholera toxin to GM1.[30,31] Our study did not evaluate the IgG deposits on the axons because nerve tissue must be examined before it undergoes axonal degeneration. Evaluation of these deposits, however, will be required to determine how IVIg prevents deposition.

In a study of GBS patients, circulating tumor necrosis factor-α (TNFα) and interleukin-1β (IL-1β) decreased after IVIg treatment but remained relatively high in untreated patients and in those treated with plasma exchange.[32] Clinical improvement of patients treated with IVIg was associated with a reduction in unbound TNFα during the acute phase of illness. In contrast, sera from GBS patients enhanced leakage in a blood–nerve barrier (BNB) model, as did anti-GM1 monoclonal antibody, TNFα, and IL-1β.[33-35] Endothelial cell junctions, which make up the BNB, are disrupted in human neuropathies associated with anti-ganglioside antibodies.[36] To clarify whether IVIg can prevent BNB dysfunction in vivo, morphologic

changes in the small vessels of the anterior roots without perfusion will need to be evaluated as to which part of the BNB is disrupted mechanically in IVIg-treated and -untreated AMAN rabbits.

IVIg may inhibit complement binding and prevent membranolytic attack complex formation.[21] This may prevent complement-mediated axonal degeneration. Interestingly, a recent study has shown that IVIg inhibits the binding of autoantibody to ganglioside, thereby preventing complement activation and being protective at motor nerve terminals.[37] IVIg may induce a blockade of the Fc receptors on macrophages by saturating, altering, or down-regulating the affinity of these receptors.[21] Blockade of Fc receptors may prevent macrophage-mediated axonal degeneration. Immunohistochemical studies of complement deposition and macrophage infiltration should clarify whether these mechanisms do function in the faster recovery of AMAN rabbits treated with IVIg.

Safer therapy than blood products can be obtained by clarifying the pharmacologic mechanisms of IVIg. Intact-type immunoglobulin was superior to $F(ab')_2$ of the IgG molecule in decreasing the clinical score of EAN rats treated before onset.[11] This indicates that the Fc portion of the IgG molecule is the more important for EAN therapeutics. Whether the $F(ab')_2$ or Fc portion is as effective as intact-type Ig used in our AMAN model will need to be examined. This will provide more information on the mechanisms of therapeutic action and facilitate development of new drugs. As an example, if the Fc portion of IgG is effective in the AMAN model, its active part can be identified. Moreover, if treatment with synthetic peptides of the active part in the Fc portion is successful in our AMAN model, then cheaper and safer peptide treatments should prove of future clinical use.

Acknowledgment

The authors thank Ms. M. Okazaki for clinical scoring, Ms. Y. Tsuchiya for serologic assays, and Ms. Y. Ueno for the treatments.

References

1. Hughes RAC, Hadden RDM, Gregson NA, Smith KJ. Pathogenesis of Guillain-Barré syndrome. J Neuroimmunol 1999;100:74–97.
2. Asbury AK, McKhann GM. Changing views of Guillain-Barré syndrome. Ann Neurol 1997;41:287–288.
3. Feasby TE, Gilbert JJ, Brown WF, et al. An acute axonal form of Guillain-Barré polyneuropathy. Brain 1986;109:1115–1126.
4. Griffin JW, Li CY, Ho TW, et al. Guillain-Barré syndrome in northern China: the spectrum of neuropathological changes in clinically defined cases. Brain 1995;118:577–595.
5. Griffin JW, Li CY, Ho TW, et al. Pathology of the motor-sensory axonal Guillain-Barré syndrome. Ann Neurol 1996;39:17–28.
6. McKhann GM, Cornblath DR, Griffin JW, et al. Acute motor axonal neuropathy: a frequent cause of acute flaccid paralysis in China. Ann Neurol 1993;33:333–342.
7. Yuki N, Yamada M, Koga M, et al. Animal model of axonal Guillain-Barré syndrome induced by sensitization with GM1 ganglioside. Ann Neurol 2001;49:712–720.
8. Plasma Exchange/Sandoglobulin Guillain-Barré Syndrome Trial Group. Randomised trial of plasma exchange, intravenous immunoglobulin, and combined treatments in Guillain-Barré syndrome. Lancet 1997; 349:225–230.
9. van der Meché FGA, Schmitz PIM, Dutch Guillain-Barré Study Group. A randomized trial comparing intravenous immune globulin and plasma exchange in Guillain-Barré syndrome. N Engl J Med 1992;326: 1123–1129.
10. Gabriel CM, Gregson NA, Redford EJ, Davies M, Smith KJ, Hughes RAC. Human immunoglobulin ameliorates rat experimental autoimmune neuritis. Brain 1997;120:1533–1540.
11. Miyagi F, Horiuchi H, Nagata I, et al. Fc portion of intravenous immunoglobulin suppresses the induction of experimental allergic neuritis. J Neuroimmunol 1997;78:127–131.
12. Crawford TO, Hsieh ST, Schryer BL, Glass JD. Prolonged axonal survival in transected nerves of C57BL/Ola mice is independent of age. J Neurocytol 1995;24:333–340.
13. Yuki N, Tagawa Y, Irie F, Hirabayashi Y, Handa S. Close association of Guillain-Barré syndrome with antibodies to minor monosialogangliosides GM1b and GM1α. J Neuroimmunol 1997;74:30–34.
14. Jacobs BC, van Doorn PA, Schmitz PIM, et al. *Campylobacter jejuni* infections and anti-GM1 antibodies in Guillain-Barré syndrome. Ann Neurol 1996;40:181–187.
15. Kuwabara S, Mori M, Ogawara K, et al. Intravenous immunoglobulin therapy for Guillain-Barré syndrome with IgG anti-GM1 antibody. Muscle Nerve 2001;24:54–58.
16. Hadden RDM, Cornblath DR, Hughes RAC, et al. Electrophysiological classification of Guillain-Barré syndrome: clinical associations and outcome. Ann Neurol 1998;44:780–788.
17. Kuwabara S, Yuki N, Koga M, et al. IgG anti-GM1 antibody is associated with reversible conduction failure and axonal degeneration in Guillain-Barré syndrome. Ann Neurol 1998;44:202–208.
18. Willison HJ, Yuki N. Peripheral neuropathy and anti-glycolipid antibodies. Brain 2002;125:2597–2625.
19. Chaudhry V, Corse AM, Cornblath DR, et al. Multifocal motor neuropathy. Response to human immune globulin. Ann Neurol 1993;33:237–242.
20. Nobile-Orazio E, Meucci N, Barbieri S, Carpo M, Scarlato G. High-dose intravenous immunoglobulin therapy in multifocal motor neuropathy. Neurology 1993;43:537–544.
21. Dalakas MC. Mechanism of action of IVIg and therapeutic considerations in the treatment of acute and chronic demyelinating neuropathies. Neurology 2002;59(suppl 6):S13–S21.
22. Yu Z, Lennon VA. Mechanism of intravenous immune globulin therapy in antibody-mediated autoimmune diseases. N Engl J Med 1999;340: 227–228.
23. Enders U, Toyka KV, Hartung H-P, Gold R. Failure of intravenous immunoglobulin (IVIg) therapy in experimental autoimmune neuritis (EAN) of the Lewis rat. J Neuroimmunol 1997;76:112–116.
24. Hafe-Macko C, Hsieh ST, Li CY, et al. Acute motor axonal neuropathy: an antibody-mediated attack on axolemma. Ann Neurol 1996;40:635–644.
25. Susuki K, Nishimoto Y, Yamada M, et al. Acute motor axonal neuropathy rabbit model: immune attack on nerve root axons. Ann Neurol 2003;54:383–388.
26. Sheikh KA, Deerinck TJ, Ellisman MH, Griffin JW. The distribution of ganglioside-like moieties in peripheral nerves. Brain 1999;122:449–460.
27. Ogino M, Orazio N, Latov N. IgG anti-GM1 antibodies from patients with acute motor neuropathy are predominantly of the IgG1 and IgG3 subclasses. J Neuroimmunol 1995;58:77–80.
28. Yuki N, Ichihashi Y, Taki T. Subclass of IgG antibody to GM1 epitope-bearing lipopolysaccharide of *Campylobacter jejuni* in patients with Guillain-Barré syndrome. J Neuroimmunol 1995;60:161–164.
29. Buchwald B, Ahangari R, Weishaupt A, Toyka KV. Intravenous immunoglobulins neutralize blocking antibodies in Guillain-Barré syndrome. Ann Neurol 2002;51:673–680.
30. Malik U, Oleksowicz L, Latov N, Cardo LJ. Intravenous γ-globulin inhibits binding of anti-GM1 to its target antigen. Ann Neurol 1996;39: 136–139.
31. Yuki N, Miyagi F. Possible mechanism of intravenous immunoglobulin treatment on anti-GM1 antibody-mediated neuropathies. J Neurol Sci 1996;139:160–162.
32. Sharief MK, Ingram DA, Swash M, Thompson EJ. IV immunoglobulin reduces circulating proinflammatory cytokines in Guillain-Barré syndrome. Neurology 1999;52:1833–1838.
33. Iwasaki T, Kanda T, Mizusawa H. Effects of pericytes and various cytokines on integrity of endothelial monolayer originated from blood–nerve barrier: an in vitro study. J Med Dent Sci 1999;46:31–40.
34. Kanda T, Iwasaki T, Yamawaki M, Tai T, Mizusawa H. Anti-GM1 antibody facilitates leakage in an in vitro blood–nerve barrier model. Neurology 2000;55:585–587.
35. Kanda T, Yamawaki M, Mizusawa H. Sera from Guillain-Barré patients enhance leakage in a blood–nerve barrier model. Neurology 2003; 60:301–306.
36. Kanda T, Yamawaki M, Iwasaki T, Mizusawa H. Glycosphingolipid antibodies and blood–nerve barrier in autoimmune demyelinative neuropathy. Neurology 2000;54:1459–1464.
37. Jacobs BC, O'Hanlon GM, Bullens RW, Veitch J, Plomp JJ, Willison HJ. Immunoglobulins inhibit pathophysiological effects of anti-GQ1b-positive sera at motor nerve terminals through inhibition of antibody binding. Brain 2003;126:2220–2234.

Carbohydrate mimicry between human ganglioside GM1 and *Campylobacter jejuni* lipooligosaccharide causes Guillain–Barré syndrome

Nobuhiro Yuki*†, Keiichiro Susuki*, Michiaki Koga*, Yukihiro Nishimoto*, Masaaki Odaka*, Koichi Hirata*, Kyoji Taguchi‡, Tadashi Miyatake‡, Koichi Furukawa§, Tetsuji Kobata¶, and Mitsunori Yamada‖

*Department of Neurology and ¶Division of Immunology, Institute for Medical Science, Dokkyo University School of Medicine, Shimotsuga, Tochigi 321-0293, Japan; ‡Department of Neuroscience, Showa Pharmaceutical University, Machida City, Tokyo 194-8543, Japan; §Department of Biochemistry II, Nagoya University School of Medicine, Nagoya City, Aichi 466-0065, Japan; and ‖Department of Pathology, Brain Research Institute, Niigata University, Niigata City, Niigata 951-8585, Japan

Edited by Michael Sela, Weizmann Institute of Science, Rehovot, Israel, and approved June 15, 2004 (received for review April 5, 2004)

Molecular mimicry between microbial and self-components is postulated as the mechanism that accounts for the antigen and tissue specificity of immune responses in postinfectious autoimmune diseases. Little direct evidence exists, and research in this area has focused principally on T cell-mediated, antipeptide responses, rather than on humoral responses to carbohydrate structures. Guillain–Barré syndrome, the most frequent cause of acute neuromuscular paralysis, occurs 1–2 wk after various infections, in particular, *Campylobacter jejuni* enteritis. Carbohydrate mimicry [Galβ1–3GalNAcβ1–4(NeuAcα2–3)Galβ1-] between the bacterial lipooligosaccharide and human GM1 ganglioside is seen as having relevance to the pathogenesis of Guillain–Barré syndrome, and conclusive evidence is reported here. On sensitization with *C. jejuni* lipooligosaccharide, rabbits developed anti-GM1 IgG antibody and flaccid limb weakness. Paralyzed rabbits had pathological changes in their peripheral nerves identical with those present in Guillain–Barré syndrome. Immunization of mice with the lipooligosaccharide generated a mAb that reacted with GM1 and bound to human peripheral nerves. The mAb and anti-GM1 IgG from patients with Guillain–Barré syndrome did not induce paralysis but blocked muscle action potentials in a muscle–spinal cord coculture, indicating that anti-GM1 antibody can cause muscle weakness. These findings show that carbohydrate mimicry is an important cause of autoimmune neuropathy.

Molecular mimicry is one mechanism by which infectious agents may trigger an immune response against autoantigens. Many reports have presented findings consistent with the mimicry hypothesis, but none have convincingly demonstrated that mimicry is an important mechanism in the development of autoimmune disease in humans (1). Although several examples of molecular mimicry between microbial and self-components are known, in most cases the epidemiological relationship between autoimmune disease and microbial infection has not been established. In other cases, moreover, no replicas of human autoimmune disease have been obtained by immunizing with the mimic of an infectious agent. Replicas associated with definite, epidemiological evidence of microbial infection are required to test the molecular mimicry theory of the development of autoimmune diseases.

Guillain–Barré syndrome (GBS), the prototype of postinfectious autoimmune diseases, ranks as the most frequent cause of acute flaccid paralysis (2). The Gram-negative bacterium *Campylobacter jejuni*, a leading cause of acute gastroenteritis in humans, is the most frequent antecedent pathogen. Epidemiological studies, which established the relationship between GBS and antecedent *C. jejuni* infection, showed that one-fourth to one-third of GBS patients develop the syndrome after being infected. GBS was considered a demyelinating disease of the peripheral nerves, but the existence of primary "axonal GBS" has been confirmed and is now widely recognized (3, 4). Ganglioside GM1 is an autoantigen for IgG Abs in patients with axonal GBS subsequent to *C. jejuni* enteritis (2, 5). *C. jejuni* strains isolated from such patients have a lipooligosaccharide (LOS) with a GM1-like structure (2, 6).

To verify that molecular mimicry between an environmental agent and the peripheral nerves causes GBS, we sensitized animals with *C. jejuni* LOS and produced a replica of human GBS, generated anti-GM1 mAb by immunization with the LOS, and determined the distribution of GM1 in human spinal nerve roots. As further proof that an autoimmune reaction causes neuromuscular disease, we showed that anti-GM1 mAb blocked muscle action potentials in a muscle–spinal cord coculture.

Methods

Preparation of *C. jejuni* LOS. The GM1-like LOS (Fig. 1*a*) was prepared from the *C. jejuni* strain (CF 90-26) isolated from a GBS patient (6) as described (7) with minor modifications. A 5-g sample of freeze-dried bacteria was suspended in 25 ml of 50 mM PBS (pH 7.0) containing 5 mM EDTA. The suspension was stirred by a shearing mixer and ultra-high-speed homogenizer (Physcotron, Microtec Nition, Chiba, Japan), after which 100 mg of hen egg lysozyme (Worthington) was added, and the whole stirred overnight at 4°C. The suspension was kept at 37°C for 20 min and then stirred again as above. The volume of the suspension was increased to 100 ml with 50 mM PBS (pH 7.0) combined with 20 mM $MgCl_2$, after which 100 μg each of ribonuclease A and DNase I (Worthington) was added. The suspension was incubated for 60 min at 37°C and then for 60 min at 60°C. After being stirred in the shearing mixer and homogenizer, the suspension was kept in a 70°C water bath for 10 min. An equal volume of 90% phenol that had been heated to 70°C was added, and the whole was homogenized for 5 min. The homogenate was rapidly cooled in an ice-water bath for 15 min and then centrifuged at 2,000 × *g*. The upper aqueous layer was removed, dialyzed against distilled water for 3 d, and then extensively centrifuged (105,000 × *g* for 16 h). The gel-like pellet obtained as the *C. jejuni* LOS was freeze-dried until used.

Western Blotting. *Escherichia coli* K12, D31m4 (Re) LOS and *Salmonella minnesota* R595 (Re) LOS were purchased from List Biological Laboratories (Campbell, CA). A 2-μg portion of each bacterial LOS was separated on a 15% tricine-SDS-polyacrylamide gel (SPU-15S series, Atto Corporation, Tokyo) (8), and each was

This paper was submitted directly (Track II) to the PNAS office.

Abbreviations: CFA, complete Freund's adjuvant; GBS, Guillain–Barré syndrome; KLH, *keyhole lympet hemocyanin*; LOS, lipooligosaccharide.

†To whom correspondence should be addressed at: Department of Neurology, Dokkyo University School of Medicine, Kitakobayashi 880, Mibu, Shimotsuga, Tochigi 321-0293, Japan. E-mail: yuki@dokkyomed.ac.jp.

www.pnas.org/cgi/doi/10.1073/pnas.0402391101

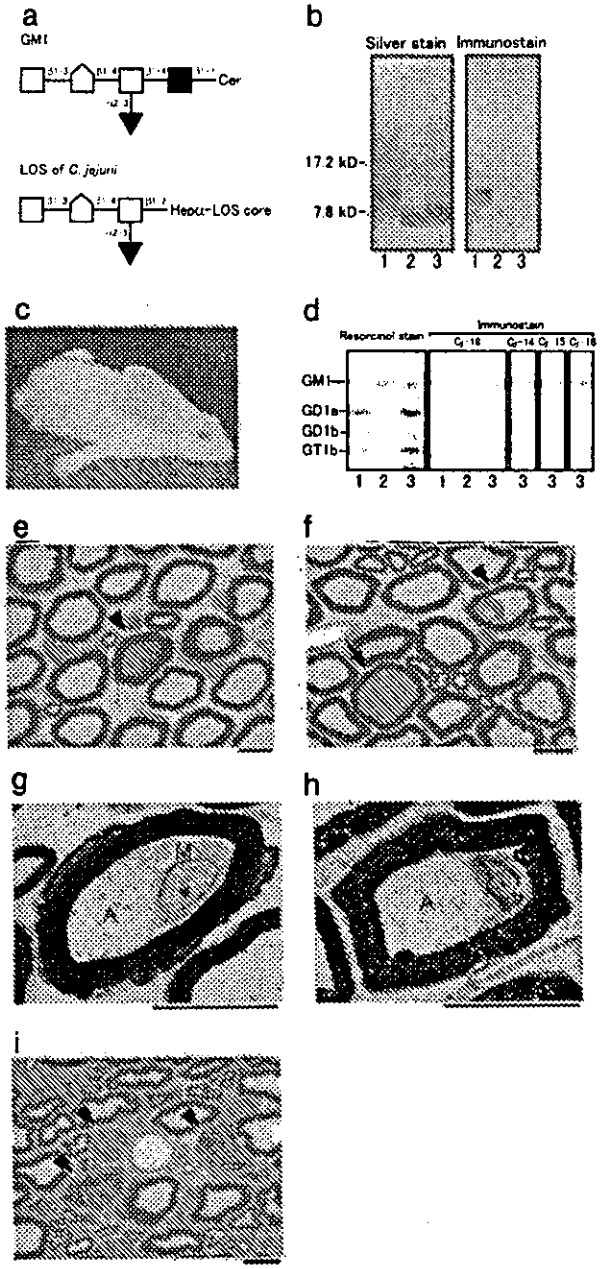

Fig. 1. Rabbit GBS model sensitized with *C. jejuni* LOS. (*a*) Carbohydrate mimicry of GM1 ganglioside by the LOS of *C. jejuni* (CF 90-26) from a GBS patient. GM1 is located in the nerve cell membrane. The LOS that mimics GM1 is in the outer part of the cell wall of *C. jejuni*. □, Galactose; ○, *N*-acetylgalactosamine; ■, glucose; ▼, *N*-acetylneuraminic acid; Cer, ceramide; Hep, heptose. (*b*) Presence or absence of the GM1 epitope in bacterial LOS-immunized rabbits. Cholera toxin B subunit reacts with the *C. jejuni* LOS (lane 1) but not with *E. coli* K12 LOS (lane 2) or *S. minnesota* R595 LOS (lane 3). (*c*) Rabbit with flaccid limb weakness induced by sensitization with *C. jejuni* LOS. Rabbit Cj-18 lays splayed out, all extremities extended, head on the floor, instead of sitting upright in the usual compact, hunched posture. (*d*) Anti-ganglioside Ab from rabbits that developed limb weakness after sensitization with *C. jejuni* LOS. Of the bovine brain gangliosides, plasma IgG from rabbit Cj-18 binds to GM1 (lane 1), isolated GM1 from bovine brain (lane 2), and GM1 from rabbit peripheral nerve (lane 3). The IgGs are from rabbits Cj-14, Cj-15, and Cj-16, and the GM1 is from rabbit peripheral nerve (lane 3). (*e–h*) Macrophages in nerve fibers. Shown are cross sections of the cauda equina from rabbit Cj-18. (*e* and *f*) Toluidine blue stain. Macrophages are present in the nerve fibers (arrowheads). The initial degenerated axon stage also is shown (arrow in *f*). Demyelination and remyelination are rare, and no inflammatory cells exist in the endoneurium. (*g* and *h*) Electron micrographs of nerve fibers with macrophage infiltration. The nerve fiber in *g* is the same as in *e*. Macrophages (M) occupy the periaxonal space between the atrophic axons (A) and the surrounding myelin sheaths, which appear almost normal. (Scale bars = 10 μm.) (*i*) Wallerian-like degeneration of nerve fibers. Shown are cross sections of the sciatic nerve from rabbit Cj-14 killed 39 days after onset. Toluidine blue stain was used. Myelin ovoids produced by Wallerian-like degeneration of the myelinated fibers are present (arrowheads). (Scale bar = 10 μm.)

blotted on a polyvinylidene difluoride membrane (Atto Corporation), which then was incubated for 2 h at 4°C with the peroxidase-conjugated cholera toxin B subunit (List Biological Laboratories). Binding was made visible with 4-chloro-1-naphtol.

Rabbit Immunization. Male Japanese white rabbits (Kbs:JW), weighing 2.0–2.5 kg, obtained from Oriental Bioservice Kanto (Ibaraki, Japan), were immunized as described (9) with minor modifications. A 2.5- or 10-mg portion of the *C. jejuni* LOS was dissolved in 0.5 ml of *keyhole lympet hemocyanin* (KLH) (2 mg/ml; Sigma) in PBS, after which 0.5 ml of complete Freund's adjuvant (CFA) (Sigma) was added, and the mixture was emulsified. A 1-ml sample of the *C. jejuni* LOS emulsion was injected s.c. in the back at 3-wk intervals until limb weakness developed or 12 mo had passed since the first inoculation. Control rabbits were injected under the same protocol with 10 mg of *E. coli* LOS or of *S. minnesota* LOS or without the LOS. The rabbits were checked daily for clinical signs, and plasma samples taken weekly by ear vein puncture.

TLC Immunostaining and ELISA. Total gangliosides were extracted from the sciatic nerves of normal rabbits and humans, and TLC immunostaining was done as described (9). In brief, the peripheral nerve gangliosides, authentic GM1, bovine brain ganglioside mixture (Cronassial; Fidia, Padova, Italy), and each LOS were layered on TLC plates. The plates were developed then overlaid with plasma from the rabbits or from a GBS patient from whom *C. jejuni* (CF 90-26) had been isolated and the anti-GM1 mAb. Last, they were incubated with peroxidase-conjugated anti-rabbit (Nordic, Tilburg, The Netherlands), anti-human (Dako, Glostrup, Denmark), or anti-mouse IgG Abs. Rabbit anti-GM1 Ab titers were tested by ELISA as described (9).

Pathological and Immunohistochemical Studies of Rabbit Peripheral Nerves. The lumbar spinal nerve root, cauda equina, and sciatic nerve specimens were evaluated pathologically, as described (9). For electron microscopy, ultrathin sections cut from tissue fragments embedded in Epon 812 resin were stained with uranyl acetate and lead citrate and then examined in a Hitachi-7100 electron microscope (Hitachi, Tokyo). In the immunohistochemical study, the nerve root, cauda equina, sciatic nerve, and tibial nerve specimens were stained with peroxidase-conjugated protein G (Sigma) as reported (9).

Generation of Anti-GM1 mAb. Mice lacking the functional gene for β1,4-*N*-acetylgalactosaminyltransferase (GM2/GD2 synthase; EC 2.4.1.92) were raised, and their genotypes were determined as described (10). Those mice did not express complex gangliosides including GM1. They were immunized i.p. four times at 2-wk intervals with 50 μg of *C. jejuni* LOS dissolved in 50 μl of KLH solution and then mixed with 50 μl of CFA. Three days after the final immunization with 50 μg of LOS in 50 μl of PBS, splenocytes were fused with P3/NS1/1-Ag4-1 myeloma cells (Health Science Research Resources Bank, Osaka). Cloning was done with a hybridoma-cloning kit (ClonaCell-HY; StemCell Technologies, Vancouver, BC, Canada). Culture supernatants

underwent an ELISA (9) with GM1 (Sigma) and anti-mouse IgG Ab (Sigma) to obtain hybridomas that secrete anti-GM1 IgG mAb. The mAb isotype produced by the hybridomas was tested with a mouse monoclonal isotyping kit (Amersham Pharmacia). The mAb produced with an i-MAb mAb production kit (Diagnostic Chemicals, Charlottetown, PE, Canada) was purified by protein G affinity chromatography according to the manufacturer's instructions (Amersham Pharmacia).

Immunohistochemistry of Human Spinal Nerve Roots. Anti-GM1 IgG from a GBS patient (Patient 1, ref. 5) was purified by affinity chromatography (11) then biotinylated with a FluoReporter MiniBiotin-XX Protein Labeling Kit (F-6347) (Molecular Probes). Spinal nerve roots without pathological changes were obtained at autopsy from an 82-year-old woman who died of bronchopneumonia. In the immunohistochemistry study, cryostat sections (6 μm thick) from snap-frozen nerve tissues were fixed with cold acetone and immunostained first with the biotinylated human anti-GM1 IgG then the avidin-biotin-peroxidase complex (ABC) in a Vectastain ABC kit (Vector Laboratories). In mouse anti-GM1 mAb, biotinylated horse anti-mouse IgG (Vector Laboratories) was the secondary Ab. Diaminobenzidine was the chromogen. After immunostaining, sections were counterstained with hematoxylin. For the negative controls, the first Abs were omitted or replaced with normal sera.

For immunoelectron microscopy, nerve roots obtained at autopsy were fixed in 4% paraformaldehyde in 0.1 M PBS (pH 7.4), dehydrated in a graded dimethylformamide series at −25°C, and embedded in LR White resin (London Resin, Berkshire, U.K.). Ultrathin sections were cut and mounted on nickel grids. After incubation with 10% normal goat serum for 10 min, the sections were incubated overnight at 4°C with the mouse anti-GM1 mAb. After being washed with PBS, the sections were incubated for 30 min at room temperature with goat anti-mouse IgG conjugated to 15-nm gold particles (British BioCell International, Cardiff, U.K.). They then were washed with PBS and incubated with 2% glutaraldehyde in 0.1 M sodium cacodylate buffer (pH 7.4). After being washed with distilled water, the sections were stained with uranyl acetate and lead citrate and examined in a Hitachi H-7100 electron microscope. For the negative controls, the primary Ab was replaced with normal mouse serum.

Muscle Action Potentials in a Rat Muscle–Spinal Cord Coculture. This was done as described (12). After 1 wk of coculture, the innervated muscle specimens were placed in an experimental chamber (35-mm Petri dish) on the stage of an inverted light microscope (IX-70; Olympus, Tokyo). The chamber (volume, 1 ml) was perfused continually with culture medium at the rate of 2–3 ml/min. Glass microelectrodes filled with 3 M KCl that had a tip resistance of 80–120 MΩ were used to record spontaneous muscle action potentials. Ten microliters of anti-GM1 mAb (GB2, 1 mg/ml), mouse IgG2bκ (MOPC-141, 1 mg/ml; Cappel, Aurora, OH), sera samples from patients who had GBS with anti-GM1 IgG, myasthenia gravis, or amyotrophic lateral sclerosis, and from normal controls with and without complement inactivation, or purified anti-GM1 IgG were added in a bath application. Electrical activity recorded by electrodes connected to a microelectrode amplifier (MEZ-8301; Nihon Kohden, Tokyo) was displayed on an oscilloscope (VC-11; Nihon Kohden). Data were transferred to a computer through an A-D converter (Digidata-1200 Interface; Axon Instruments, Union City, CA) and stored. The spontaneous action potential was low-pass filtered at 1 kHz. All experiments were performed at 33 ± 1°C.

Passive Transfer in Mice. Male C57BL/6 mice (12 wk of age; SLC, Hamamatsu, Japan) were injected intravenously with 1 mg of the anti-GM1 mAb or 10 mg of the purified human anti-GM1 IgG. The mice were checked daily for clinical sings. Sera and nerve tissue were obtained 2 wk after the injection. Mouse and human anti-GM1 Ab titers were tested by ELISA, and the cauda equina was stained with peroxidase-conjugated protein G (Sigma) as described (9).

Results

Induction of Paralyzed Rabbits. None of the 10 controls inoculated only with KLH and CFA every 3 wk showed limb weakness until 12 mo after the first inoculation, whereas 4 of the 10 rabbits immunized with 2.5 mg of *C. jejuni* LOS, KLH, and CFA developed limb weakness sooner. Two rabbits (Cj-9 and Cj-6) developed flaccid paresis of the hind limbs 215 and 216 d after the initial inoculation and tetraparesis the next day. They were unable to lift their heads and bodies, respectively, 5 and 4 d after onset. Two other rabbits (Cj-1 and Cj-4) developed tetraparesis 133 and 329 d after the initial inoculation, but weakness was mild during the course of the illness.

The cholera toxin B subunit (a specific ligand for GM1-oligosaccharide) bound strongly to the *C. jejuni* LOS, but did not react with *E. coli* K12 LOS or *S. minnesota* R595 LOS (Fig. 1*b*). None of the control rabbits inoculated with 10 mg of *E. coli* LOS ($n = 5$) or *S. minnesota* LOS ($n = 5$) showed limb weakness until 12 mo after the first inoculation. In contrast, all eight rabbits immunized with 10 mg of the *C. jejuni* LOS, KLH, and CFA developed limb weakness earlier. One rabbit (Cj-18) developed flaccid paresis of the hind limbs 64 d after the initial inoculation and tetraparesis 7 d after its onset (Fig. 1*c* and Movie 1, which is published as supporting information on the PNAS web site). The others (Cj-11 to Cj-17) developed tetraparesis 227, 47, 176, 172, 40, 64, and 128 d, respectively, after the initial inoculation. Quadriparesis and respiratory paresis developed and progressed rapidly in three rabbits (Cj-11, Cj-13, and Cj-17), causing death 2, 15, and 1 d, respectively, after onset of limb weakness. One rabbit (Cj-15), however, had a monophasic course like that of patients with GBS. After onset, limb weakness worsened for 8 d, reached a plateau, and then lessened from day 16.

Induction of Anti-GM1 Antibody. TLC with immunostaining showed that, as to rabbit peripheral nerve gangliosides, plasma IgG Abs from the paralyzed rabbits reacted strongly with the GM1 (Fig. 1*d*) and with the *C. jejuni* LOS (data not shown), whereas neither *E. coli* LOS nor *S. minnesota* LOS induced anti-GM1 Abs in the rabbits. The IgG Abs from the paralyzed rabbits did not react with GD1a, GD1b, or GT1b (Fig. 1*d*). Anti-GM1 IgM antibodies were detected in the eight paralyzed rabbits 2–4 wk after their first sensitization with *C. jejuni* LOS. Anti-GM1 IgG antibodies were detected in these rabbits 4–6 wk after their first inoculation, and the titers gradually increased by repeated immunizations. Six of the eight rabbits developed flaccid paresis within 3 wk (median, 1 wk) after the peak anti-GM1 IgG titer was reached (range, 2,000–32,000; median, 8,000), but the titers did not correlate with the severity.

Pathological Findings in Diseased Rabbits. The spinal nerve roots of rabbit Cj-18 killed 11 d after onset had few nerve fibers showing Wallerian-like degeneration, whereas the nerve roots showed occasional macrophages within the periaxonal spaces surrounded by almost intact myelin sheaths (Fig. 1 *e–h*). Axons of these nerve fibers had various degrees of degeneration. Sciatic nerve specimens from the paralyzed rabbits showed more severe Wallerian-like degeneration than did the proximal nerve roots (Fig. 1*i*). Demyelination and remyelination were rare, and no inflammatory cells were present in the endoneurium. Furthermore, protein G bound selectively to some axons in the cauda equina of rabbit Cj-12, indicating that IgG deposits were on those axons (data not shown). In contrast, no significant changes were found in the brains or spinal cords of any of the paralyzed rabbits.

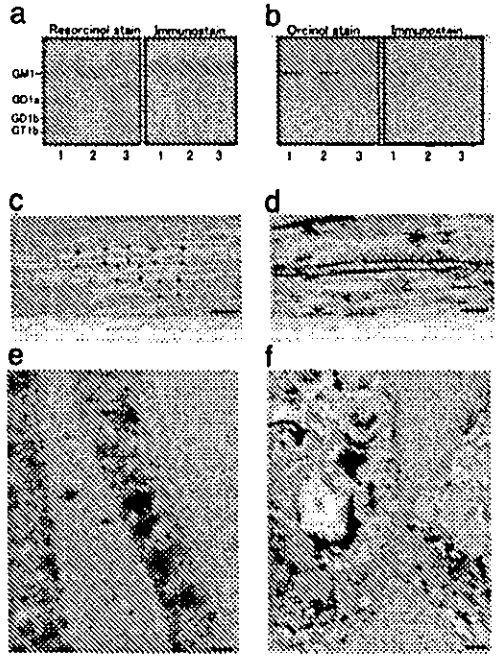

Fig. 2. Immunoreactivity of anti-GM1 mAb. (*a* and *b*) Binding specificity of the mAb (GB2) generated by *C. jejuni* LOS. (*a*) Of the bovine brain gangliosides, it recognizes GM1 (lane 1), the GM1 isolated from bovine brain (lane 2), and the GM1 of human peripheral nerve (lane 3). (*b*) The mAb reacts with the *C. jejuni* LOS (lane 1) but not with *E. coli* K12 LOS (lane 2) or *S. minnesota* R595 LOS (lane 3). (*c–f*) GM1 immunoreactivity in the anterior nerve roots of the human lumbar cord with the biotin-conjugated anti-GM1 IgG from a GBS patient (*c*) and the anti-GM1 mAb (*d–f*). (*c* and *d*) Labeling is present in the myelin sheaths of both large and small myelinated axons. (*e*) GM1 antigenicity is localized on the myelin lamellae, plasma membrane of the outer Schwann cell process, the basal lamina, and the mitochondria and some vacuoles of an axon. (*f*) Labeling also is present on Schwann cell processes surrounding the nodal region of an axon. (*c* and *d*) The immunoperoxidase method was used. (*e* and *f*) The immunogold method is indicated by 15-nm gold particles. (Scale bars = 30 μm in *c* and *d*, 1 μm in *e*, and 2 μm in *f*.)

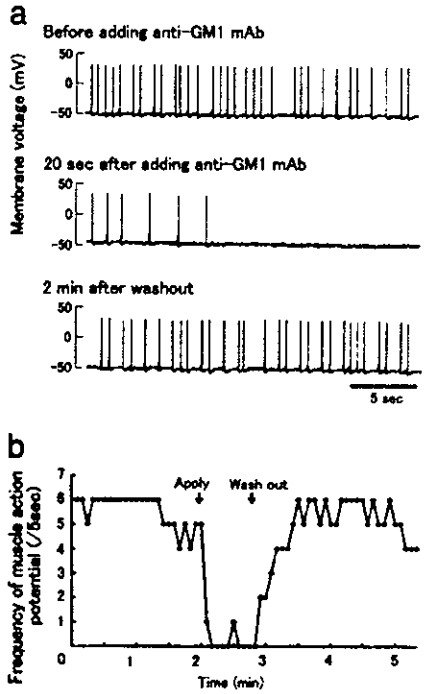

Fig. 3. Biologic activity of anti-GM1 mAb. (a) Blockade of muscle action potentials by anti-GM1 mAb in muscle–spinal cord cocultured cells. (*b*) Time course of inhibition of spontaneous muscle action potentials by anti-GM1 mAb recovery after washout. The number of potentials was measured every 5 s. Arrows show times of the anti-GM1 mAb addition and exchange of the bath solution.

Characteristics of mAb GB2. A clone with anti-GM1 IgG activity (GB2), subclass IgG2bκ, was obtained. TLC immunostaining showed it reacted strongly with the GM1 in a bovine brain ganglioside mixture that included GM1, GD1a, GD1b, and GT1b (Fig. 2*a*) and with the *C. jejuni* LOS (Fig. 2*b*). An ELISA showed that GB2 reacted with GM1 but not with gangliosides GM2, GD2, GalNAc-GD1a, GT1a, or GQ1b, evidence of its highly restricted binding specificity for GM1. Anti-GM1 mAb was therefore used in our study. TLC immunostaining confirmed that our anti-GM1 mAb reacted strongly with the GM1 in human peripheral nerve gangliosides (Fig. 2*a*).

Localization of Anti-GM1 Ab Binding in Human Spinal Nerve Roots. The immunohistochemistry of the anterior roots of the human spinal cord showed that the anti-GM1 IgG from the patient with GBS subsequent to *C. jejuni* enteritis reacted with the myelin sheaths of both large and small myelinated fibers (Fig. 2*c*). Fine dot-like staining of the axons also was detectable. Immunostaining with mAb gave similar results (Fig. 2*d*) and visibly labeled Schwann cell cytoplasms. Fibroblasts or collagen fibrils were negative for GM1. No immunostaining occurred when the first Ab was omitted or replaced with normal mouse serum. Immunoelectron microscopy with mAb confirmed the presence of GM1 antigenicity on the myelin lamellae on the outermost cell membrane of Schwann cell processes and on the basal lamina. Labeling was present along the axolemmas of axons and on occasional vesicles and mitochondria in the axoplasm (Fig. 2*e*). Labeling of Schwann cell processes around unmyelinated axons also was visible. At the nodes of Ranvier immunoreactivity occurred on Schwann cell processes covering the nodal regions of axons (Fig. 2*f*). No immunostaining took place when the first Ab was replaced with normal mouse serum.

Biologic Activity of Anti-GM1 Ab in Muscle–Spinal Cord Cocultures. After 1 wk of coculture, asynchronous contractions of several individual muscle fibers had occurred on formation of neuromuscular junctions (Fig. 3*a* and Movie 2, which is published as supporting information on the PNAS web site). Muscle action potential frequency was 1.3 ± 0.54 per s and amplitude was 75.2 ± 6.4 mV (n = 6). Anti-GM1 mAb prolonged the muscle action potential intervals at the neuromuscular junctions, beyond which potentials were inhibited (Fig. 3 and Movie 3, which is published as supporting information on the PNAS web site). This inhibition did not occur with the isotype-matched control Ab. The blockade of muscle action potentials by anti-GM1 mAb was fully reversed after a wash with the culture medium (Fig. 3). Sera from 11 patients who had GBS associated with anti-GM1 IgG after *C. jejuni* enteritis and from seven patients with myasthenia gravis also blocked the muscle action potentials, whereas sera from seven patients with amyotrophic lateral sclerosis and seven healthy control subjects did not. GBS sera with complement inactivation inhibited potentials, and purified anti-GM1 IgG from the GBS patient (patient 1, ref. 5) also blocked them.

Passive Transfer in Mice. None of the mice injected with mouse (n = 5) and human (n = 5) anti-GM1 IgG showed limb weakness

until 2 wk after the i.v. injection. Mouse and human anti-GM1, respectively, were detected in their sera obtained at the time of killing. No protein G bound to axons in the cauda equina of the mice, indicating that no IgG deposits were present on those axons.

Discussion

If molecular mimicry by an infectious agent is the trigger of an autoimmune response leading to an autoimmune disease, several conditions must be satisfied: (*i*) the pathogen must be associated with the onset of the symptoms or disease in a convincing number of cases; (*ii*) a clinically detectable immune response to the pathogen must be demonstrable, at least at disease onset, which response must be shown to cross-react with host antigens of the affected tissues; and (*iii*) the pathology of the disease must be consistent with the immune response (13). As discussed below, these conditions have been established for GBS subsequent to *C. jejuni* infection, proof that GM1 mimicry by *C. jejuni* does cause GBS. Many *C. jejuni* strains actually have been isolated from GBS patients at the onset of limb weakness (14). Patients with axonal GBS subsequent to *C. jejuni* enteritis have anti-GM1 IgG, and the titers peak early in the disease, followed by a gradual decline (5). *C. jejuni* LOSs from GBS isolates have a tetrasaccharide structure consistent with GM1 mimicry (2, 6).

Several research groups have failed to induce neuropathy by sensitization with *C. jejuni* LOS with GM1 epitope. Rats immunized with *C. jejuni* LOS only showed an IgM response to GM1 (15). Anti-GM1 IgG has been induced in rabbits by sensitization with the LOS from the *C. jejuni* reference strain obtained from a patient with enteritis and the LOSs from GBS-associated strains, but no muscle weakness was observed (16, 17): The New Zealand White rabbits were immunized with a smaller amount of LOS and no KLH, and the observation period may have been too short. Because induction rates of the GM1-inoculated GBS model depend on species or breed susceptibility and the immunization procedure used (18), Japanese white rabbits were injected repeatedly with KLH and 2.5 mg of *C. jejuni* LOS bearing a GM1-like structure. Four of the 10 rabbits developed weakness that was associated with anti-GM1 IgG. Next, a larger amount of the LOS was injected. All eight rabbits immunized with 10 mg of the LOS developed limb weakness, and muscle weakness progressed rapidly. One rabbit had a monophasic course similar to the clinical course of patients with GBS. GM1 is expressed on rabbit peripheral nerve axons (9), and all the paralyzed rabbits had IgG Abs to GM1 in their peripheral nerve gangliosides. Macrophages within the periaxonal space surrounded by an intact myelin sheath are the pathological substrate of axonal GBS (3). This finding was confirmed in the nerve roots of rabbit Cj-18. Sciatic nerve specimens from the paralyzed rabbits showed Wallerian-like degeneration. Demyelination and remyelination were rare, and no T cell infiltration occurred. IgG was deposited on some axons in the cauda equina of rabbit Cj-12. These findings, compatible with the features of human axonal GBS (3, 4), provide evidence that the rabbits inoculated with *C. jejuni* LOS constitute a valid GBS model. This definitive replica of a human autoimmune disease produced by immunizing with the mimic of the infectious agent associated with epidemiological evidence of microbial infection has not been reported previously.

Whereas most GBS patients develop limb weakness within 3 wk after *C. jejuni* infection, the paralyzed rabbits required several inoculations with GM1-like LOS and with GM1 (9). In contrast, the anti-GM1 IgG titers correlated with the disease onset in the inoculated rabbits and in the GBS patients (5). The inflammatory response in GBS may be triggered by either activation of complement or leukocytes. The induction of inflammation is triggered by the concerted action of complement and FcγR (19). Anti-GM1 IgG from GBS patients induces leukocyte effector functions such as degranulation and phagocytosis (20). We have shown in the GM1-inoculated rabbits that anti-GM1 IgG efficiently induces such inflammatory reactions at the onset, whereas it dose not before the onset (W.-L. van der Pol and N.Y., unpublished data). These findings suggest that a large amount of anti-GM1 IgG associated with the effector functions is required for the development of limb weakness. The pathogenic antibody could be induced easily in the patients with GBS subsequent to *C. jejuni* infection but not in the rabbits immunized by GM1 and *C. jejuni* LOS, probably because of their diversity of the anti-GM1 response. The reason should be elucidated by further studies.

LOS is composed of oligosaccharide and lipid A. Several lines of evidence support an GM1 oligosaccharide rather than lipid A structure for the *C. jejuni* LOS that has importance in the development of GBS. *E. coli* K12 LOS and *S. minnesota* R595 LOS do not carry the GM1 epitope. Sensitization of those LOSs that carry lipid A did not induce anti-GM1 Abs in the rabbits, evidence that anti-GM1 IgG is not a result of polyclonal B cell stimulation. None of the rabbits developed limb weakness. In contrast, a GBS model has been established that uses inoculation with GM1, which carries a ceramide moiety but not lipid A (9). Sensitization with GM1 induced anti-GM1 IgG in rabbits, who developed limb weakness. The pathology is identical with that of human axonal GBS and with that of paralyzed rabbits inoculated with *C. jejuni* LOS. IgG Ab to GQ1b also is associated with Fisher syndrome, which is characterized by ophthalmoplegia, ataxia, and areflexia (21). That syndrome is considered a variant of GBS because some patients develop GBS during the clinical course of Fisher syndrome, but patients with Fisher syndrome typically do not develop limb weakness or have anti-GM1 IgG. *C. jejuni* isolates from Fisher syndrome have an LOS with GQ1b epitope (22). Five rabbits were sensitized with 10 mg of *C. jejuni* (CF 93–6) LOS bearing GQ1b epitope, but none of them developed limb weakness (N.Y., unpublished data). This indirect evidence shows that the nature of the GM1-oligosaccharide structure is important for the development of GBS.

We injected *C. jejuni* LOS into the mice lacking GM1 (immune naïve hosts) and obtained an IgG-class mAb that is highly specific for GM1. The anti-GM1 mAb bound to the GM1 of human peripheral nerve gangliosides on a TLC plate. A point worth noting is that GM1 is expressed in both the peripheral and central nervous systems but that sensitization with GM1 or the GM1-like LOS produces only peripheral neuropathy. This characteristic seems to occur because the blood–brain barrier that protects the brain and spinal cord is much tighter than the blood–nerve barrier. Electrophysiological, immunohistochemical, and pathological study findings show that the initial lesion in axonal GBS may be localized in the spinal nerve roots (23, 24). The reason may be that nerve roots are vulnerable because they lack a blood–nerve barrier. The cholera toxin B subunit stains both the nodes of Ranvier and paranodal Schwann cells in human spinal roots (25), which we confirmed with the anti-GM1 mAb and anti-GM1 IgG from a GBS patient. Similar immunohistochemical results with mAbs were obtained for spinal nerve roots in rabbits (data not shown). GM1 was expressed on axons of the anterior nerve roots in both humans and rabbits, which nerve roots seem to be the initial lesion in axonal GBS. The clinical, pathological, and immunological features of the paralyzed rabbits sensitized with the *C. jejuni* LOS were very similar to those of axonal GBS. We therefore speculate that the pathogenesis of axonal GBS subsequent to *C. jejuni* enteritis is as follows: (*i*) Infection by *C. jejuni* carrying a GM1-like LOS induces high production of anti-GM1 IgG in patients who have a particular immunogenetic background, (*ii*) the autoantibody binds to GM1 expressed on motor nerve axons in the spinal roots, and (*iii*) the deposited IgG recruits macrophages into the periaxonal space where they attack the axon and Wallerian-like degeneration occurs.

Limb weakness in some GBS patients is quickly cured by plasmapheresis, indicating that autoantibody causes physiological conduction failure in the motor nerves before any pathological change occurs (26). The nerve terminal lacks a blood–nerve barrier; therefore, Abs have easy access to neuronal membranes, the presumed sites of injury. In a mouse phrenic nerve–diaphragm preparation, the IgG from GBS patients produced neuromuscular blockade in a complement-independent manner (27). We added anti-GM1 mAb to rat muscle–spinal cord cocultures, and it blocked muscle action potentials at the neuromuscular junctions. This blockade was fully reversed after a wash with the culture medium, consistent with the clinical observation that in GBS plasma exchange induces rapid recovery. The anti-GM1 IgG present in GBS subsequent to *C. jejuni* enteritis also blocked muscle action potentials and was complement-independent. Although the blockade mechanism needs to be clarified, these findings are consistent with anti-GM1 IgG being biologically active and pathogenic and producing muscle weakness directly in patients with GBS. In mice, systemic injection of mouse or human anti-GM1 IgG did not induce paralysis and IgG binding to the peripheral nerves, although the amount of antibody injected and/or the duration of treatment might not be sufficient. Passive transfer of axonal degeneration in rat peripheral nerves, however, was produced by intraneural injection of human and rabbit anti-GM1 IgGs associated with complements (M. Kamijo and N.Y., unpublished data). These findings suggest that other factors such as tumor necrosis factor-α and IL-1β, which enhance leakage in the blood–nerve barrier (28), are required to induce clinical and pathological disease by the systemic injection. Circulating tumor necrosis factor-α and IL-1β increase in GBS patients (29), and this increase could occur also in our active immunization model using CFA.

In conclusion, this study has verified that molecular mimicry between an environmental agent and the peripheral nerves causes GBS. Molecular mimicry is an important mechanism in the development of human autoimmune diseases. Research on molecular mimicry and autoimmunity principally has focused on T cell-mediated, antipeptide responses, rather than on Ab responses to carbohydrate structures (1). Our findings show that carbohydrate mimicry between GM1 and the *C. jejuni* LOS induces the production of pathogenic autoantibodies and the development of GBS. This new concept that carbohydrate mimicry can cause an autoimmune disease provides a clue to the resolution of the pathogenesis of other immune-mediated diseases.

We thank S. Koike and K. Yamaguchi (Institute for Medical Science, Dokkyo University School of Medicine) for their technical assistance. This work was supported in part by a grant-in-aid for Scientific Research (B) (KAKENHI 14370210 to N.Y.) from the Ministry of Education, Culture, Sports, Science and Technology of Japan; a Health Science Research grant (Research on Brain Science) from the Ministry of Health and Welfare of Japan; and Human Frontier Science Program Grant RGP 38/2003.

1. Marrack, P. J. & Kotzin, B. L. (2001) *Nat. Med.* **7**, 899–905.
2. Yuki, N. (2001) *Lancet Infect. Dis.* **1**, 29–37.
3. McKhann, G. M., Cornblath, D. R., Griffin, J. W., Ho, T. W., Li, C. Y., Jiang, Z., Wu, H. S., Zhaori, G., Liu, Y., Jou, L. P., *et al.* 1993. *Ann. Neurol.* **33**, 333–342.
4. Hafer-Macko, C., Hsieh, S.-T., Li, C. Y., Ho, T. W., Sheikh, K., Cornblath, D. R., McKhann, G. M., Asbury, A. K. & Griffin J. W. (1996) *Ann. Neurol.* **40**, 635–644.
5. Yuki, N., Yoshino, H., Sato, S. & Miyatake, T. (1990) *Neurology* **40**, 1900–1902.
6. Yuki, N., Taki, T., Inagaki, F., Kasama, T., Takahashi, M., Saito, K., Handa, S. & Miyatake, T. (1993) *J. Exp. Med.* **178**, 1771–1775.
7. Johnson, K. G. & Perry, M. B. (1976) *Can. J. Microbiol.* **22**, 29–34.
8. Schägger, H. & von Jagow, G. (1987) *Anal. Biochem.* **166**, 368–379.
9. Yuki, N., Yamada, M., Koga, M., Odaka, M., Susuki, K., Tagawa, Y., Ueda, S., Kasama, T., Ohnishi, A., Hayashi, S., *et al.* (2001) *Ann. Neurol.* **49**, 712–720.
10. Takamiya, K., Yamamoto, A., Furukawa, K., Yamashiro, S., Shin, M., Okada, M., Fukumoto, S., Haraguchi, M., Takeda, N., Fujimura, K., *et al.* (1996) *Proc. Natl. Acad. Sci. USA* **93**, 10662–10667.
11. Hirabayashi, Y., Suzuki, T., Suzuki, Y., Taki, T., Matsumoto, M., Higashi, H. & Kato, S. (1983) *J. Biochem. (Tokyo)* **94**, 327–330.
12. Taguchi, K., Utsunomiya, I., Ren, J., Yoshida, N., Aoyagi, H., Nakatani, Y., Ariga, T., Usuki, S., Yu, R. K. & Miyatake, T. (2004) *Neurochem. Res.* **29**, 953–960.
13. Davies, J. M. (1997) *Immunol. Cell Biol.* **75**, 113–126.
14. Yuki, N., Takahashi, M., Tagawa, Y., Kashiwase, K., Tadokoro, K. & Saito, K. (1997) *Ann. Neurol.* **42**, 28–33.
15. Wirguin, I., Briani, C., Suturkova-Milosevic, L., Fisher, T., Della-Latta, P., Chalif, P. & Latov, N. (1997) *J. Neuroimmunol.* **78**, 138–142.
16. Ritter, G., Fortunato, S. R., Cohen, L., Noguchi, Y., Bernard, E. M., Stockert, E. & Old, L. J. (1996) *Int. J. Cancer* **66**, 184–190.
17. Ang, C. W., Endtz, H. P., Jacobs, B. C., Laman, J. D., de Klerk, M. A., van der Meché, F. G. & van Doorn, P. A. (2000) *J. Neuroimmunol.* **104**, 133–138.
18. Yuki, N., Mori, I. & Susuki, K. (2002) *Ann. Neurol.* **52**, 128–129.
19. Ravetch, J. V. (2002) *J. Clin. Invest.* **110**, 1759–1761.
20. van Sorge, N. M., van den Berg, L. H., Geleijns, K. P. W., van Strijp, J. A., Jacobs, B. C., van Doorn, P. A., Wokke, J. H. J., van de Winkel, J. G. J., Leusen, J. H. W. & van der Pol, W.-L. (2003) *Ann. Neurol.* **53**, 570–579.
21. Chiba, A., Kusunoki, S., Shimizu, T. & Kanazawa, I. (1992) *Ann. Neurol.* **31**, 677–679.
22. Yuki, N., Taki, T., Takahashi, M., Saito, K., Yoshino, H., Tai, T., Handa, S. & Miyatake, T. (1994) *Ann. Neurol.* **36**, 791–793.
23. Griffin, J. W., Li, C. Y., Macko, C., Ho, T. W., Hsieh, S.-T., Xue, P., Wang, F. A., Cornblath, D. R., McKhann, G. M. & Asbury, A. K. (1996) *J. Neurocytol.* **25**, 33–51.
24. Susuki, K., Nishimoto, Y., Yamada, M., Baba, M., Ueda, S., Hirata, K. & Yuki, N. (2003) *Ann. Neurol.* **54**, 383–388.
25. Sheikh, K. A., Deerinck, T. J., Ellisman, M. H. & Griffin, J. W. (1999) *Brain* **122**, 449–460.
26. Kuwabara, S., Yuki, N., Koga, M., Hattori, T., Matsuura, D., Miyake, M. & Noda, M. (1998) *Ann. Neurol.* **44**, 202–208.
27. Buchwald, B., Toyka, K. V., Zielasek, J., Weishaupt, A., Schweiger, S. & Dudel, J. (1998) *Ann. Neurol.* **44**, 913–922.
28. Iwasaki, T., Kanda, T. & Mizusawa, H. (1999) *J. Med. Dent. Sci.* **46**, 31–40.
29. Sharief, M. K., Ingram, D. A., Swash, M. & Thompson, E. J. (1999) *Neurology* **52**, 1833–1838.

ELSEVIER

Journal of the Neurological Sciences 219 (2004) 139–145

Journal of the Neurological Sciences

www.elsevier.com/locate/jns

Clinical correlates of serum anti-GT1a IgG antibodies

Takahide Nagashima, Michiaki Koga, Masaaki Odaka, Koichi Hirata, Nobuhiro Yuki*

Department of Neurology, Dokkyo University School of Medicine, Kitakobayashi 880, Mibu, Shimotsuga, Tochigi 321-0293, Japan

Received 18 July 2003; received in revised form 18 December 2003; accepted 5 January 2004

Abstract

Patients with the pharyngeal-cervical-brachial variant (PCB) of Guillain–Barré syndrome (GBS) have anti-GT1a IgG with or without GQ1b reactivity, whereas those with Fisher syndrome (FS) or Bickerstaff's brainstem encephalitis (BBE) have anti-GQ1b IgG antibodies which cross-react with GT1a. The nosological relationship between these conditions has yet to be established. To investigate the relationships between each manifestation and between clinical features and the coexistence of anti-GQ1b IgG, we reviewed neurological signs present during illnesses of 140 patients who had anti-GT1a IgG. Based on our criteria, FS was diagnosed for 64 (46%) patients, GBS for 22 (16%), BBE for 14 (10%), and PCB for 6 (4%). Overlapping conditions were diagnosed for some patients: FS and GBS (5%), PCB and FS (5%), BBE and GBS (4%), and PCB and BBE (1%). Patients who initially had bulbar palsy developed not only PCB but FS or BBE. The population of anti-GT1a-positive patients frequently had ophthalmoplegia, ataxia, and areflexia, whereas the subpopulation who had anti-GT1a IgG without GQ1b reactivity frequently had preceding diarrhea as well as oropharyngeal, neck, and limb weakness. Patients with anti-GT1a IgG presented a variety of clinical conditions, indicative of a continuous clinical spectrum. A major part of this clinical variation was due to the coexistence of anti-GQ1b IgG. The presence of a common autoantibody (anti-GT1a IgG) and overlapping illnesses suggests that PCB is closely related not only to GBS but to FS and BBE as well.

Keywords: Guillain–Barré syndrome; Pharyngeal-cervical-brachial variant; Anti-GT1a antibody; Anti-GQ1b antibody; Fisher syndrome; Bickerstaff's brainstem encephalitis

1. Introduction

Guillain–Barré syndrome (GBS) is characterized by the acute onset of limb weakness. Bulbar palsy, which causes respiratory failure or aspiration and occasionally may require intubation, has been reported in two-fifths of GBS patients studied [1]. Ropper [2] described three patients, in whom oropharyngeal, neck, and shoulder weaknesses progressed acutely. He called this regional variant "pharyngeal-cervical-brachial weakness resembling botulism or diphtheria" and, elsewhere, proposed diagnostic criteria [1].

Cumulative evidence supports the speculation that anti-ganglioside antibodies function in the development of GBS and its variants [3]. A patient developed the pharyngeal-cervical-brachial variant (PCB) after an intramuscular injection of bovine ganglioside mixture [4], indicative that anti-ganglioside antibodies also have a pathogenetic role in the development of PCB. Anti-GT1a IgG antibodies with and without GQ1b reactivity have been detected in patients who have acute oropharyngeal palsy [5,6], PCB [7–9], or GBS [10–12]. On the other hand, anti-GQ1b IgG antibody with anti-GT1a reactivity has been found in patients who have Fisher syndrome (FS), Bickerstaff's brainstem encephalitis (BBE), acute ophthalmoparesis (AO) without ataxia, or ataxic GBS [13–15]. The nosological relationship between PCB and these other conditions, however, has yet to be established. The aim of our study was to clarify the clinical features of anti-GT1a-positive patients who had various neurological disorders and the relationships between PCB and related conditions.

2. Materials and methods

2.1. Patients

A sequential retrospective study was made of 2,148 consecutive patients with various neurological disorders.

* Corresponding author. Tel.: +81-282-86-1111x2360; fax: +81-282-86-5884.

E-mail address: yuki@dokkyomed.ac.jp (N. Yuki).

0022-510X/$ - see front matter © 2004 Elsevier B.V. All rights reserved.
doi:10.1016/j.jns.2004.01.005

Serum samples were obtained from patients who had been referred to our laboratory for serum anti-ganglioside antibody testing by Japanese university and district general hospitals between August 1999 and November 2001.

2.2. Enzyme-linked immunosorbent assay

Serum IgG antibodies to GT1a, GQ1b, GM1, GM1b, GM2, GD1a, GalNAc-GD1a, GD1b, and GT1b were measured routinely by an enzyme-linked immunosorbent assay (ELISA) as reported elsewhere [16]. Absorbance values at 492 nm were calculated by subtracting the optical densities obtained for wells without antigen. In this study, serum was considered positive for anti-ganglioside antibodies when the absorbance value was 0.5 or higher at the dilution of 1:500 because, as reported elsewhere [17], this high cut-off level gives high specificity.

2.3. Clinical feature analysis

Information on antecedent illnesses, initial symptoms, neurological signs and respiratory distress during the illness, and cerebrospinal fluid (CSF) findings were obtained from patients who had anti-GT1a IgG. The neurological signs assessed were consciousness disturbance, blepharoptosis, ophthalmoplegia, facial weakness, bulbar palsy, nuchal weakness, distribution of limb weakness, deep tendon reflexes, pathological reflexes, ataxia, sensory impairment, and autonomic dysfunction. The patients' clinical features were reviewed by one of the authors (T.N.) by means of questionnaires and their medical records at discharge obtained from each primary physician. When the medical records did not contain adequate information, follow-up faxes were sent to the physicians. Patients with anti-GT1a antibodies were divided into subgroups according to the other antibodies present, after which the clinical features of the subgroups were compared.

2.4. Diagnostic criteria

Diagnosis of GBS was based on the established criteria [18]. Diagnoses of FS, BBE, AO, overlapping FS and GBS (FS/GBS), and overlapping BBE and GBS (BBE/GBS) were based on our published criteria [15]. The diagnostic criteria used for PCB are given in Table 1. Patients who had ophthalmoplegia and ataxia, in addition to the clinical features of PCB, were considered to have overlapping PCB and FS (PCB/FS). Those who had consciousness disturbance, hyperreflexia, or hemisensory disturbance, as well as ophthalmoplegia, ataxia, and the clinical features of PCB were considered to have overlapping PCB and BBE (PCB/BBE). The presence of extensor plantar responses did not exclude a diagnosis of GBS [18] or a variant if the other clinical features were typical.

Table 1
Diagnostic criteria for the pharyngeal-cervical-brachial variant of Guillain–Barré syndrome

Clinical features
(1) Progressive weakness predominant in the neck, shoulders, proximal arms, and oropharyngeal muscles over 1–3 weeks
(2) Areflexia or hyporeflexia, at least in the arms
(3) Lower limb strength of 5 or 4 on the Medical Research Council scale
Features strongly supportive of the diagnosis
(1) A history of infection symptoms within 4 weeks before the onset of neurological symptoms
(2) CSF albuminocytological dissociation
(3) Abnormal motor nerve conduction or late responses
Differential diagnoses
botulism, diphtheria, myasthenia gravis, polymyositis, multiple sclerosis, vascular disease, vasculitis, brainstem tumor, toxic or metabolic neuropathy
Appendix
Extensor plantar responses do not exclude the diagnosis if other clinical features are typical.
Patients with both ophthalmoparesis and ataxia are diagnosed as having an overlap of the pharyngeal-cervical-brachial variant and Fisher syndrome.
Patients with CNS involvement (consciousness disturbance, hyperreflexia, or hemisensory disturbance) together with ophthalmoparesis and ataxia are diagnosed as having an overlap of the pharyngeal-cervical-brachial variant and Bickerstaff's brainstem encephalitis.

CSF = cerebrospinal fluid; CNS = central nervous system.

2.5. Statistical analysis

Differences in proportions were examined by the χ^2 or Fisher's exact (two-tailed) test. Differences in medians were examined by the Mann-Whitney U test. A difference of $p<0.05$ was considered significant. Ninety-five percent confidence interval was calculated from the odds ratios (OR). Statistical analyses were done with Statcel software (OMS, Saitama, Japan).

3. Results

3.1. Clinical features of patients with anti-GT1a IgG antibodies

Anti-GT1a IgG antibodies were positive in 140 patients (median age, 40; 77 men, 63 women), 12 of whom were reported elsewhere [11]. Table 2 shows the clinical profiles during illness. Eighty-nine percent of the patients had an antecedent illness (upper respiratory tract infectious symptoms alone, 65%; diarrhea alone, 8%; both, 16%). The most frequent initial symptom was diplopia, the second unsteady gait; both cardinal symptoms of FS.

Most patients had muscular weakness of acute and monophasic progression. Frequent signs occurring during illness were the triad of FS. Eighty-nine percent of the patients had hypo- or areflexia, 85% external ophthalmoparesis, and 71% cerebellar-type ataxia (truncal alone, 15%; limb alone, 2%; both, 54%). Half of the patients had neck or limb weakness, and 37% of them showed proximal-dominant, 20% distal-dominant, and 43% diffuse limb weakness. Fifty-four percent

Table 2
Clinical profiles of patients with anti-GT1a IgG antibody

	Total	FS	GBS	BBE	AO	PCB	FS/GBS	BBE/GBS	PCB/FS	PCB/BBE	Unclassified
Patients (*n*)	140	64	22	14	7	6	7	5	7	2	6
Gender (men/women)	77/63	39/25	12/10	8/6	4/3	5/1	3/4	2/3	2/5	0/2	2/4
Median age (range)	40 (4–86)	40 (4–86)	32 (4–71)	41 (11–67)	34 (6–54)	63 (29–71)	60 (32–86)	47 (29–74)	35 (21–76)	47 (27–68)	36 (20–51)
Antecedent illness:	(%)	(%)	(%)	(%)	(%)	(%)	(%)	(%)	(%)	(%)	(%)
Upper respiratory infection	81	91	64	86	86	50	86	100	71	50	50
Diarrhea	24	20	27	21	43	50	14	20	43	0	17
Initial symptoms:											
Diplopia	37	50	9	29	71	0	43	20	43	0	33
Unsteady gait	21	33	0	14	0	17	29	40	0	50	17
Limb weakness	19	0	86	14	0	17	14	20	14	50	0
Photophobia	6	3	0	21	14	0	14	0	0	0	33
Rhinolalia aperta	4	3	0	0	0	33	0	0	29	0	0
Dysphagia	4	2	5	7	14	17	0	0	0	0	17
Blepharoptosis	2	3	0	0	0	0	0	0	14	0	0
Others	6	6	0	14	0	17	0	20	0	0	0
Neurological signs during illness:											
Consciousness disturbance	9	0	0	50	0	0	0	100	0	50	0
Blepharoptosis	36	39	23	50	14	0	43	40	57	100	17
Internal ophthalmoparesis	38	41	14	64	14	17	43	100	43	50	17
External ophthalmoparesis	85	100	32	100	100	33	100	100	100	100	67
Facial weakness	36	17	59	50	0	67	57	80	43	100	33
Bulbar palsy	42	20	55	43	29	100	57	100	100	100	33
Weakness of the neck or limbs:	54	28[a]	100	43[a]	0	100	100	100	100	100	50
Neck	38	11[a]	91	7[a]	0	100	43	100	100	100	33
Upper limbs	52	25[a]	95	43[a]	0	100	100	100	100	100	50
Lower limbs	44	16[a]	95	43[a]	0	50[a]	100	100	71[a]	100	33
Tendon reflex in arms:											
Brisk or normal	12	3[b]	0	50	43[b]	0	0	0	0	0	83[b]
Absent or decreased	88	97	100	50	57	100	100	100	100	100	17
Tendon reflex in legs:											
Brisk or normal	14	3[b]	5[b]	57	43[b]	17[b]	0	0	0	0	83[b]
Absent or decreased	86	97	95	43	57	83	100	100	100	100	17
Pathological reflex	8	0	0	43	0	0	0	60	14	50	0
Ataxia	71	100	0	79[c]	0	17	100	80[c]	100	100	67
Superficial sense impairment	54	61	59	36	29	17	86	60	29	100	50
Deep sense impairment	24	28	14	14	0	17	29	40	43	100	0
Autonomic dysfunction	16	8	27	29	0	17	29	40	14	50	17
CSF:											
Median cell (range) (/μl)	4 (0–176)	4 (0–67)	5 (0–72)	14 (0–161)	4 (0–5)	3 (1–24)	8 (1–25)	3 (0–176)	3 (0–3)	7 (6–7)	5 (3–6)
Median protein (range) (mg/dl)	46 (11–225)	50 (14–179)	48 (11–112)	31 (23–144)	28 (20–80)	48 (36–64)	81 (23–225)	34 (30–64)	98 (29–207)	34 (29–39)	69 (15–132)

FS = Fisher syndrome; GBS = Guillain–Barré syndrome; BBE = Bickerstaff's brainstem encephalitis; AO = acute ophthalmoparesis; PCB = pharyngeal-cervical-brachial weakness; FS/GBS = overlapping FS and GBS; BBE/GBS = overlapping BBE and GBS; PCB/FS = overlapping PCB and FS; PCB/BBE = overlapping PCB and BBE; and CSF = cerebrospinal fluid.

[a] Four or more on the Medical Research Council scale.

[b] Deep tendon reflexes were decreased in the other limb.

[c] Because of consciousness disturbance, ataxia could not be assessed in three patients with BBE and one with PCB/BBE.

had superficial sense impairment. Respiratory distress was seen in 11%, and endotracheal intubation was used for 13%. Some patients without respiratory distress also required endotracheal intubation due to severe bulbar palsy.

3.2. Diagnoses for patients with anti-GT1a IgG antibodies

Frequent diagnoses were FS and related disorders (Table 2). Some patients had an overlapping condition; FS/GBS, PCB/FS, BBE/GBS, or PCB/BBE. The illnesses of the remaining six (4%) patients were unclassified: four had acute progression of ophthalmoparesis and ataxia with preserved tendon reflexes; one acute weakness of the oropharynx, neck, and arms with preserved tendon reflexes; and one superficial sense impairment with autonomic dysfunction. Examples of PCB/FS and PCB/BBE cases are given hereafter.

3.3. Case report of PCB/FS

A 76-year-old man suffered cough, sore throat, and fever which abated over 3 days. Four days after their resolution, he experienced both rhinolalia aperta without dry mouth and numbness of the forearms (day 1). The next day he had difficulty in swallowing and was admitted to a hospital. He was mentally alert but had severe paretic dysarthria and dysphagia. The soft palate could not be raised, and pharyngeal and palatal reflexes were absent. Ocular movement was not limited. Blepharoptosis and facial weakness were absent. Muscle strength in the neck and four limbs was normal. Deep tendon reflexes were brisk in the upper limbs and normal in the lower ones. Plantar responses were indifferent. Ataxia was not present. Hypesthesia and dysesthesia of the upper limbs were present. There was no autonomic nervous dysfunction. On day 5, proximal-dominant arm weakness (3 on the MRC scale), associated with hyporeflexia in the arms was present. Nuchal weakness of 4 on the MRC scale was found on day 6. The CSF protein concentration was 23 mg/dl with 1 cell/μl on day 5. An electrophysiological study on day 6 showed delayed distal latencies and slow motor nerve conduction velocities in the median, ulnar, and tibial nerves. Conduction block was present in the median and ulnar nerves. Sensory nerve conduction showed mildly decreased potentials in all the nerves tested. Serological examinations were negative for recent *Campylobacter jejuni* or *Haemophilus influenzae* infection. An ELISA showed that the patient had IgG antibodies to GT1a (titer of 16,000) and GQ1b (2000).

GBS had been diagnosed by the primary physician, and six sessions of immunoadsorption therapy with a phenylalanine-conjugated column [19] were conducted between days 7 and 21. On day 7, he developed external ophthalmoparesis, facial weakness, and cerebellar-type ataxia. Neck and proximal arm weakness, respectively, were 2 and 3 on the MRC scale. Because of the truncal ataxia, mono-pedal stance and tandem gait were impossible. On day 10, rhinolalia and muscle weakness began to decrease. His limb power had returned to normal, but mild bulbar palsy remained on day 20. On day 6, PCB would have been the diagnosis, but PCB/FS was diagnosed instead because he showed ophthalmoparesis and ataxia on day 7.

3.4. Case report of PCB/BBE

A 27-year-old woman with no history of antecedent infectious illness experienced clumsiness and numbness of the right arm and leg (day 1). Two days later, she developed unsteady gait. On day 5, she became drowsy and had rhinolalia aperta, and so was admitted to a hospital. The neurological examination showed left blepharoptosis, bifacial weakness, and bulbar palsy. Ocular movement was disturbed in abducens gaze on the left. Neck and arm weakness was 3 on the MRC scale, but leg power was preserved. Deep tendon reflexes were absent. She was unable to walk without support because of cerebellar-type ataxia. Hypesthesia and hypalgesia were present in the right arm and leg. Urination was disturbed. EEG showed diffuse slow waves in 7–9 Hz background activities. No F wave could be elicited from the median and tibial nerves. Compound muscle action potentials of facial nerves were de-

Table 3
Diagnoses for patients with antibodies against individual gangliosides

Diagnosis	No.	IgG antibodies to :							
		GQ1b (%)	GM1 (%)	GM1b (%)	GM2 (%)	GD1a (%)	GalNAc-GD1a (%)	GD1b (%)	GT1b (%)
Total	140	94	6	21	1	14	3	11	9
FS	64	100	0	14	0	2	0	5	3
GBS	22	73	36	41	9	50	9	32	32
BBE	14	100	0	36	0	7	0	0	0
AO	7	100	0	0	0	0	0	0	14
PCB	6	83	0	33	0	33	0	17	17
FS/GBS	7	100	14	29	0	14	14	29	14
BBE/GBS	5	100	0	0	0	0	20	40	0
PCB/FS	7	100	0	29	0	14	0	0	0
PCB/BBE	2	100	0	50	0	50	0	0	0
Unclassified	6	67	0	0	0	17	0	0	17

Abbreviations as in Table 2.